JOURNAL OF GEOPHYSICAL RESEARCH, VOL. 92, NO. C12, PAGES 12,947-12,966, NOVEMBER 15, 1987

The California Current System: The Seasonal Variability of its Physical Characteristics

RONALD J. LYNN

Southwest Fisheries Center, National Marine Fisheries Service, La Jolla, California

JAMES J. SIMPSON

Scripps Institution of Oceanography, La Jolla, California

The seasonal variation of the physical characteristics and of large-scale current patterns of the California Current system is examined using harmonic analysis applied to the 23 years of California Cooperative Oceanic Fisheries Investigations data collected between 1950 and 1978. The amplitude and phasing of seasonal variation in dynamic height and the overall standard deviation of dynamic height define three domains: oceanic, coastal, and an intervening transition zone. The transition zone is a broad band centered approximately 200–300 km offshore and parallel to the coast in which the seasonal range of dynamic height is a relative minimum and the standard deviation is a maximum. It is hypothesized that recurrent mesoscale eddies and energetic meanders create this zone. Such eddies and meanders would contribute heavily to the standard deviation of dynamic height but not its seasonal variation. The transition zone is coincident with the core of flow of the California Current. A strong interaction between the core of the California Current and the mesoscale eddy field is evident. Seasonal variation in the fields of temperature, salinity, σ_t, and oxygen is related to variations in the California Current, the Inshore Countercurrent and the California Undercurrent through vertical adjustments in the density field and through changes in transport. In the undercurrent there is an especially strong relation between seasonal variations in strength of flow and the extreme values of water mass characteristics.

1. INTRODUCTION

The California Current (CC) is the eastern limb of the large-scale, anticyclonic North Pacific gyre. Except near the coast, the CC is a surface (0–300 m deep) current which carries water equatorward throughout the year along the west coast of North America to the North Equatorial Current. The average speed of the CC off the coast of California is typically less than 25 cm s^{-1} [*Reid and Schwartzlose*, 1962]. Daily average surface speeds, as high as 50 cm s^{-1}, have been observed using drifters [*Davis*, 1985]. The characteristics of the CC (i.e., low temperature, low salinity, high dissolved oxygen) change abruptly to the west, at the California Front [e.g., *Saur*, 1980]. Here, a region of complex salinity structure, a southeastward continuation of the Subarctic Frontal Zone, lies between the CC and the waters typical of the eastern North Pacific water mass [e.g., *Lynn*, 1986]. *Sverdrup et al.* [1942] use this water mass boundary as the western limit of the CC. It lies 850 to 900 km off the California coast. Near the coast (typically within 150 km), there is a seasonal change in the direction of this surface flow. Throughout the fall and winter, the direction of this narrow zone of coastal surface flow is often poleward [*Reid and Schwartzlose*, 1962; *Hickey*, 1979; *Chelton*, 1984]. We refer to this poleward flow as the Inshore Countercurrent (IC). North of Point Conception the IC is often referred to as the Davidson Current. There is inshore poleward flow along southern California and Baja California as well, and at times it is continuous about the headland at Point Conception [e.g., *Hickey*, 1979]. We prefer the general description "Inshore Countercurrent" rather than regional names for what may be a general phenomenon. (This choice is not meant to imply temporal and spatial continuity of flow.)

The California Undercurrent (CU) is considered to originate in the eastern equatorial Pacific and to flow poleward along the North American coast [*Sverdrup and Fleming*, 1941; *Reid et al.*, 1958]. *Reid* [1962, 1963], on the basis of drogue measurements, was the first to suggest that this flow might be concentrated in a relatively narrow high-speed core off both Point Conception and Baja California. *Wooster and Jones* [1970] further confirmed the existence of the high speed core off Baja California with hydrographic and direct current meter observations. *Hickey* [1979] reviewed the available observations of the CU from San Francisco to Baja California and concluded that the CU shows considerable seasonal variability in position, strength, and core depth. She relates aspects of the current field and seasonal variability to the fields of wind stress and curl of the wind stress. *Chelton* [1984] examined seasonal variability of the nearshore geostrophic velocity along California mostly limited to the region between Point Sur and Point Conception. His study attempts to relate the observation record to various models of ocean dynamics.

The water properties of these currents are determined by four water masses, each defined by its temperature, salinity, dissolved oxygen, and nutrients at the time it enters the California Current system. Pacific Subarctic water forms at high latitudes in regions of excess precipita-

Paper number 7C0607.
0148-0227/87/007C-0607$05.00

TABLE 1. Relative Comparison of Water Masses of the California Current and California Undercurrent [From *Simpson*, 1984*a*]

	T	S	O_2	Nutrients
Surface water masses (0–200 m)				
Pacific Subarctic	L	L	H	H
North Pacific Central	H	H	L	L
Coastal Upwelled	L	H	L	H
Subsurface water masses (200–500 m)				
Equatorial Pacific	H	H	L	H

L, low; H, high.

tion and heat loss. This water is entrained in the Subarctic Current and West Wind Drift, and it enters the CC near 48°N [*Pickard*, 1964]. It has relatively low temperature T, low salinity S, high dissolved oxygen O_2, and high phosphate [*Reid et al.*, 1958; *NORPAC Committee*, 1960, plates 9 and 14]. Water of Pacific Subarctic origin is still recognizable by its relatively low salinity as it leaves the CC near 25°N [*Reid et al.*, 1958]. Pacific Subarctic water gives the CC its offshore near-surface salinity minimum and high dissolved oxygen. Eastern North Pacific Central water [*Sverdrup et al.*, 1942; *Pickard*, 1964] is warm, salty, and relatively low in dissolved oxygen and nutrients [*Reid et al.*, 1958]. It enters the California Current system from the west. Equatorial Pacific water forms in the eastern tropical Pacific and has relatively high temperature, high salinity, high nutrients, and low dissolved oxygen [*Sverdrup et al.*, 1942; *Pickard*, 1964]. It enters the deeper-lying CU from the south. Upwelling within 50 km of the California coast brings relatively cold, salty, nutrient-rich, and oxygen-deficient water from depth to the surface [*Sverdrup*, 1938; *Reid et al.*, 1958]. A summary of these water properties is given in Table 1.

In this study we describe the seasonal variation of the physical characteristics and large-scale current patterns of the California Current system and their interrelationships. Although other authors have described and discussed aspects of the seasonal variation for some of its characteristics at some depth levels and for some subregions, we attempt to provide an integrated picture of the mean seasonal variation of the physical characteristics of the California Current system over the entire domain from the coast to approximately 1000 km offshore and from San Francisco to southern Baja California using data collected over the period 1950 through 1978.

2. DATA

Large-scale systematic hydrographic sampling of the California Current system was initiated in 1949 by the California Cooperative Oceanic Fisheries Investigations (CalCOFI) program. Since 1950, stations have been repeatedly occupied at varying intervals based on a geographically fixed grid. The station occupation record is given by *Eber and Wiley* [1982]. In all, over 16,000 stations have been occupied from 1950 through 1978. Those stations for which there is an accumulation of observations adequate for the determination of seasonal cycles fall in a region extending offshore to 700 km and from San Francisco to southern Baja California. The sampling grid is based on parallel lines oriented approximately perpendicular to the coast (Figure 1*a*). The separation of the lines

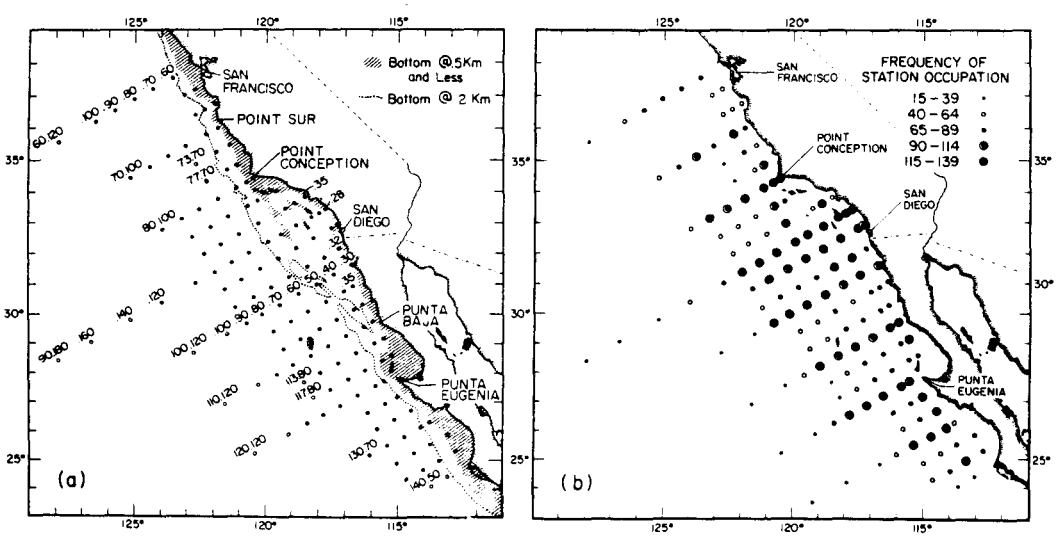

Fig. 1. (*a*) CalCOFI station pattern. Harmonic analysis was applied to data for all stations shown here. The 2000-m isobath is shown dotted. Bathymetry less than 500 m is hatched. (*b*) Record of station occupation.

and the standard spacing of stations are both 74 km. Near shore the station spacing is half or less, and at the western edge of the pattern it is sometimes double. The original grid spacing was designed upon units of nautical miles (1 n. mi = 1.852 km). Standard line/station spacing was 40 n. mi; one unit of station number equals 4 n. mi, and one unit of line number equals 12 n. mi. (In this strict notation, station lines such as 93 and 97 are actually 93.333... and 96.666... .)

Through 1964, 18-bottle Nansen casts were the standard sampling method at hydrographic stations. After 1964, salinity-temperature-depth (STD) and conductivity-temperature-depth (CTD) casts were taken alone, in conjunction with a Nansen cast, or with a few water bottle samples for calibration. In addition to measurements of temperature and salinity, determinations of oxygen concentration frequently were made. Values of the oceanographic measurements and computed parameters are interpolated to 14 standard levels (0, 10, 20, 30, 50, 75, 100, 125, 150, 200, 250, 300, 400, and 500 m).

In general, the minimum criterion for analysis of seasonal variation was a station occupancy of 40 or more (Figure 1*b*). In the heavily sampled areas near the coast and especially in the Southern California Bight, the occupancy requirement was set higher to avoid large differences between neighboring stations. Most stations near the western boundary of the CalCOFI grid have been occupied less than 40 times. Data for these latter stations may be insufficient to properly resolve seasonal variability. They are, however, included in this analysis because they provide the best available information, albeit limited, on seasonal cycles in the far offshore domain of the California Current system. The station lines numbered in whole decades (every third line in Figure 1*a*) are termed cardinal lines and generally have been occupied more frequently than the other lines. The cardinal lines were chosen for more detailed analysis in this study.

3. METHODOLOGY

We fitted harmonic curves composed of annual and semiannual components to each data record by regression analysis using the method of least squares. These curves provide an expression of the mean seasonal variation of each data record [*Lynn*, 1967; *Chelton*, 1982, 1984; *Godfrey and Ridgway*, 1985]. There are five data records at each grid point, one each for temperature, salinity, σ_t, dissolved oxygen, and dynamic height. There is a grid point for each of the 14 standard depths, at each selected station. Each harmonic curve is described by five coefficients. The coefficients are used to generate an estimate of a "mean" value of a characteristic at each standard level for any given time of the year. From these mean values we computed mean seasonal range of characteristics, days of occurrence of seasonal extremes, and mean seasonal differences between specified dates. We also computed the vertical distribution of isopleths of a characteristic versus time of year. It should be noted that a few of the figures given herein are derived from arithmetically averaged data where such maps would not differ from those produced by least squares fit to harmonics. They are noted in the captions as taken from *Lynn et al.* [1982].

Geostrophic velocities relative to 500 dbar were calculated from the station-to-station differences between the harmonic curves expressing dynamic height (see *Chelton* [1984] for a thorough analysis of the methodology). The choice of 500 dbar as the reference level is dictated by the data set. *Wyllie* [1966] shows the current field at 500 m relative to 1000 dbar to be very weak. At this level there is a relief of 1 to 2 dyn cm over the CalCOFI grid which gives an estimated flow of less than 1 cm s^{-1}. It is possible, however, that currents at 500 m may be more substantial in the vicinity of ridges and the continental slope. Geostrophic velocities are underestimated by the coarse station spacing in regions where flow consists of a narrow jet such as the CU [*Wooster and Jones*, 1970]. Hence we cannot derive the details of the narrow CU and IC flows. The spatial scale of the CalCOFI grid, however, does permit us to examine these flows in general terms.

At those coastal stations where the depth of the bottom is less than 500 m, a reference level of 500 dbar is not available. For four such stations, 80.52, 90.28, 100.30, and 130.35, we have extrapolated the offshore horizontal density gradient at levels between the deepest observed levels and 500 dbar in order to estimate the surface flow. The extrapolation method is described by *Montgomery* [1941] and *Reid and Mantyla* [1976]. In choosing this approach, we note that it is sensitive to small errors in dynamic height. Most of the vertical shear and its variability, however, occur at shallow levels, and the sensitivity to small errors in dynamic height is ameliorated by smoothing with harmonic analysis. We feel that this procedure allows us to gain insight into the large inshore variability in current structure over the continental slope.

4. RESULTS

4.1. *Dynamic Height*

Contour maps of dynamic height for the sea surface with respect to 500 dbar for four seasonal periods (Figure 2) show, to some degree, the variations in relative strength of near-surface flows. The strongest equatorward flow (CC) appears in spring and summer, whereas the strongest poleward coastal counterflow (IC) appears in fall and winter. The coastal counterflow is best organized during January; during April there is barely a vestige of this flow. By July, the Southern California Eddy has formed. This cyclonic eddy is geographically fixed about the shallow offshore banks of the Southern California Bight (Figure 1*a*). The CC has a large shoreward component just south of the international border [*Reid et al.*, 1963]. This flow divides; part flows northward as the nearshore limb of the Southern California Eddy or as the IC, and part flows southward along the coast. South of this division in flow, distributions for all seasons show a looping meander in the vicinity of Guadalupe Island (~29°N, 118°W).

Dynamic height at 200 m with respect to 500 dbar (Figure 3) shows patterns of seasonal flow similar to those at the surface. The equatorward flow is, however, considerably weaker at this level, and the poleward flow is generally broader and more coherent. The poleward flow during April is limited in extent to southern California and a short distance north of Point Conception. During most of the year off northern Baja California, a greater portion of the CC turns shoreward and then poleward at this level than at the surface.

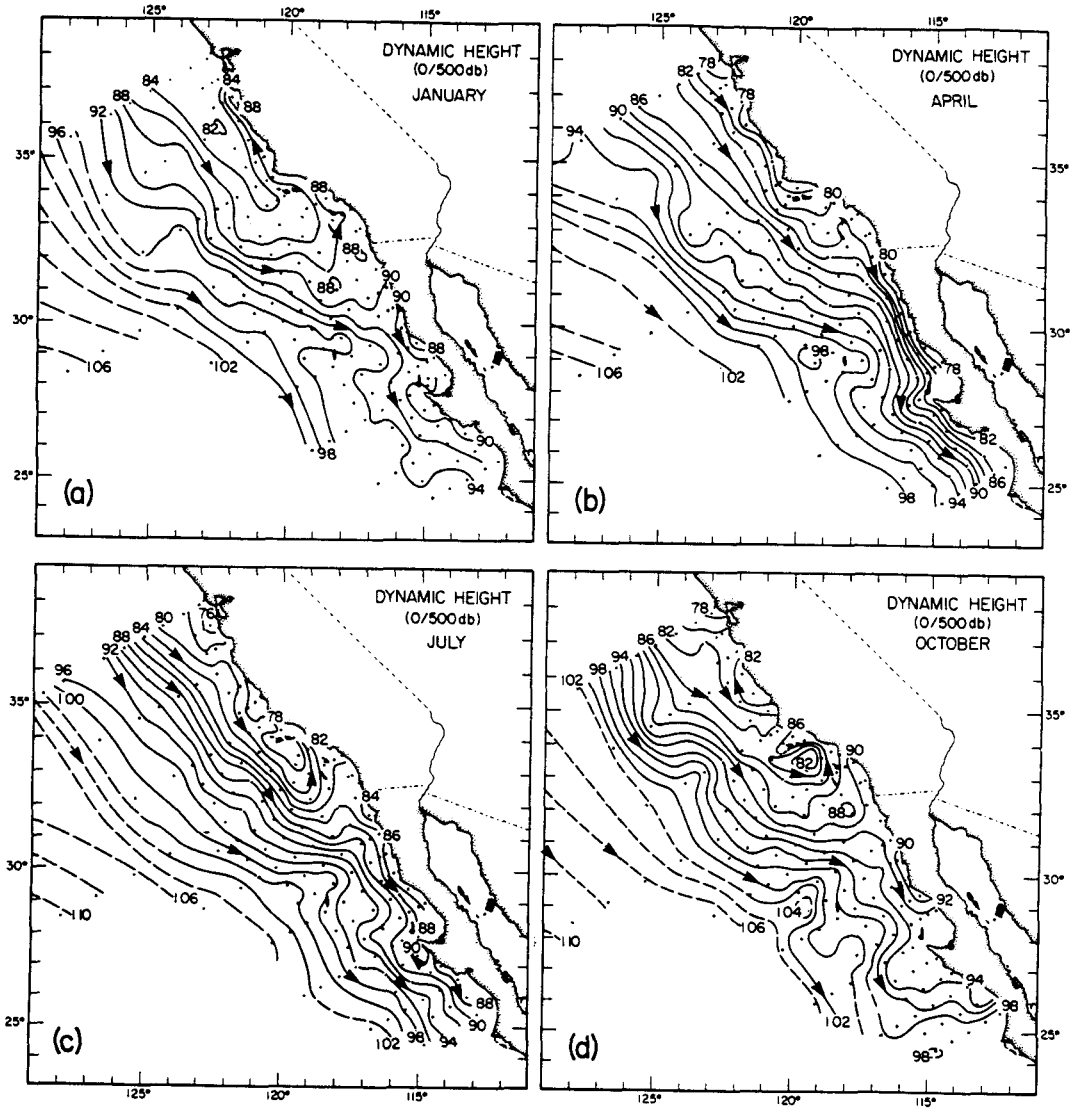

Fig. 2. Mean dynamic height (in dynamic centimeters) of the surface relative to 500 dbar for four periods (of approximately 60 days) centered about (*a*) January, (*b*) April, (*c*) July, and (*d*) October [from *Lynn et al.*, 1982]. Contour interval is 2 dyn cm.

Dynamic height also can be used to define regions where the influence and phasing of the geostrophic dynamics differ markedly. A coastal region, an offshore region, and a transition zone between them are readily identified by variations in the dynamic height of the surface with respect to 500 dbar (Figure 4). There is a seasonal tilting of the sea surface shown by the difference in dynamic height between the mean distribution for January 15 and that for July 15 (Figure 4*a*). Although the sea surface falls as much as 6 dyn cm in a band within 200 km of the coast during the first half of an average year, it rises an equivalent amount in the offshore region during the same period. Between these two regions there is a zone with little or no change in dynamic height. The full range of the seasonal variation (the harmonic highs minus the lows, regardless of date) produces a similar pattern (Figure 4*b*). The seasonal range exceeds 9 dyn cm along the coast and in the offshore region; a minimum, generally less than 5 dyn cm, forms a trough in this distribution centered approximately 200 km offshore. In the offshore region the seasonal minimum occurs in winter (Figure 4*c*). In the coastal zone it occurs some 4 months later. In the transition zone the seasonal cycle is weaker and erratic.

There is a band of high values >|4| dyn cm (the hatched area in Figure 4*d*) in the distribution of standard deviation about the overall record of dynamic height (i.e.,

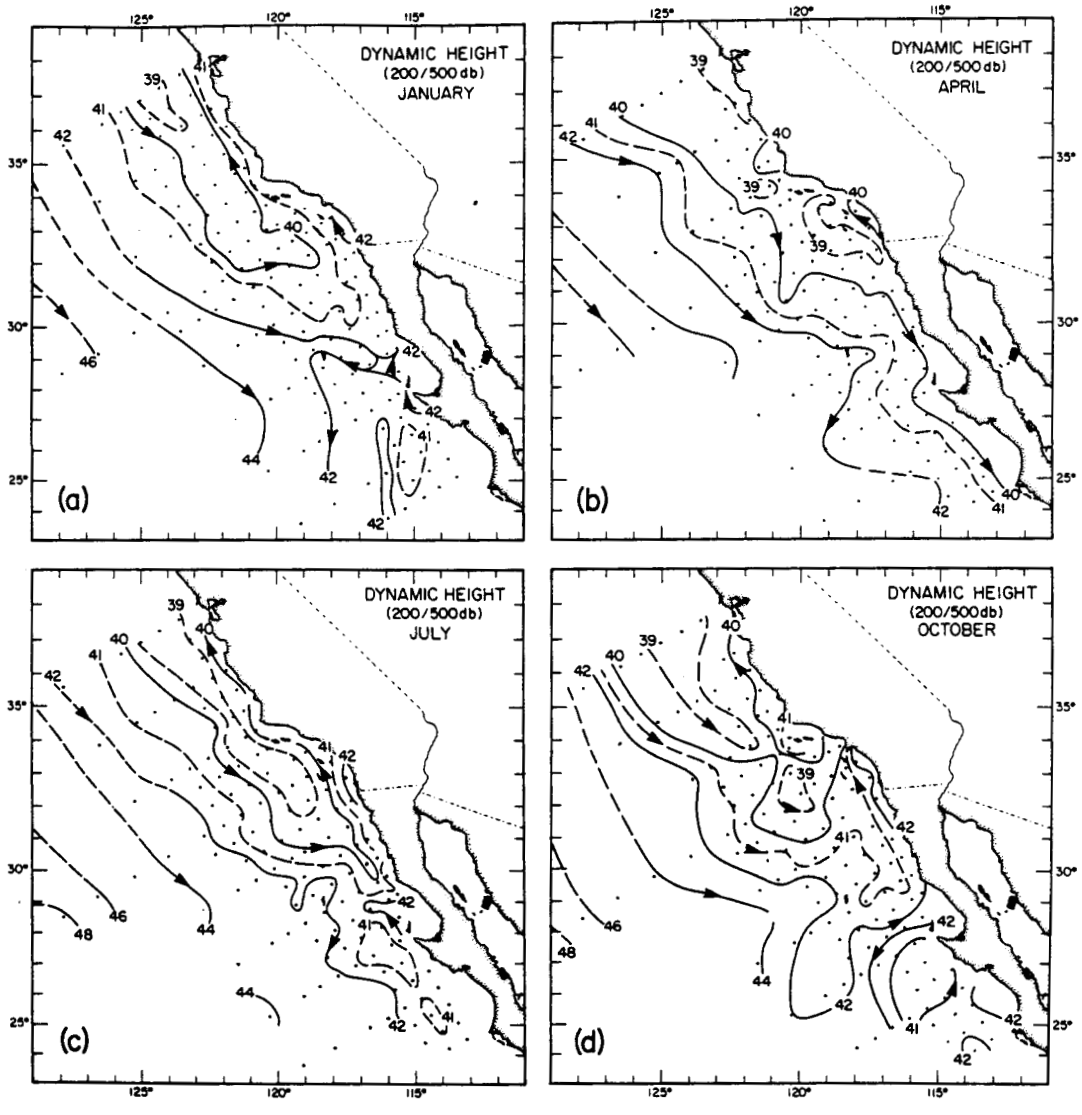

Fig. 3. The same as Figure 2 except for 200 m relative to 500 dbar. Contour interval is 1 dyn cm.

seasonal cycle not removed) in the transition zone between the coastal and offshore regimes. This band of high standard deviation in dynamic height coincides with the transition zone defined above. In general, in the zone where standard deviation in dynamic height is a maximum, its seasonal variation is a minimum.

4.2. *Surface Flow and Characteristics*

4.2.1. *California Current and Inshore Countercurrent.* Vertical sections of geostrophic velocity relative to 500 dbar along CalCOFI lines 70, 90, and 110 for odd months are given in Figures 5, 6, and 7, respectively. *Chelton* [1984] presents a figure similar to Figure 5, but his values differ from ours. His notation of station spacing given in kilometers is in error (too low) by the ratio of statute miles to nautical miles, which possibly accounts for his values appearing of the order of 10 to 20% higher than ours. (His conclusions, however, were not affected by this error.) *Lynn et al.* [1982] also give similar figures which were derived from arithmetic means.

Several generalizations about the California Current and Inshore Countercurrent can be made from the velocity sections (Figures 5, 6, and 7). The CC is a relatively shallow flow; the maximum velocity occurs at or near the surface. Flow exceeding 4 cm s^{-1} often does not extend below 150 m. In some seasons it occurs in bands defined by one or two pairs of stations separated by 75 to 150 km. The swiftest mean equatorward flow exceeds 20 cm s^{-1} at the surface of the inshore station pair of line 110 (Fig-

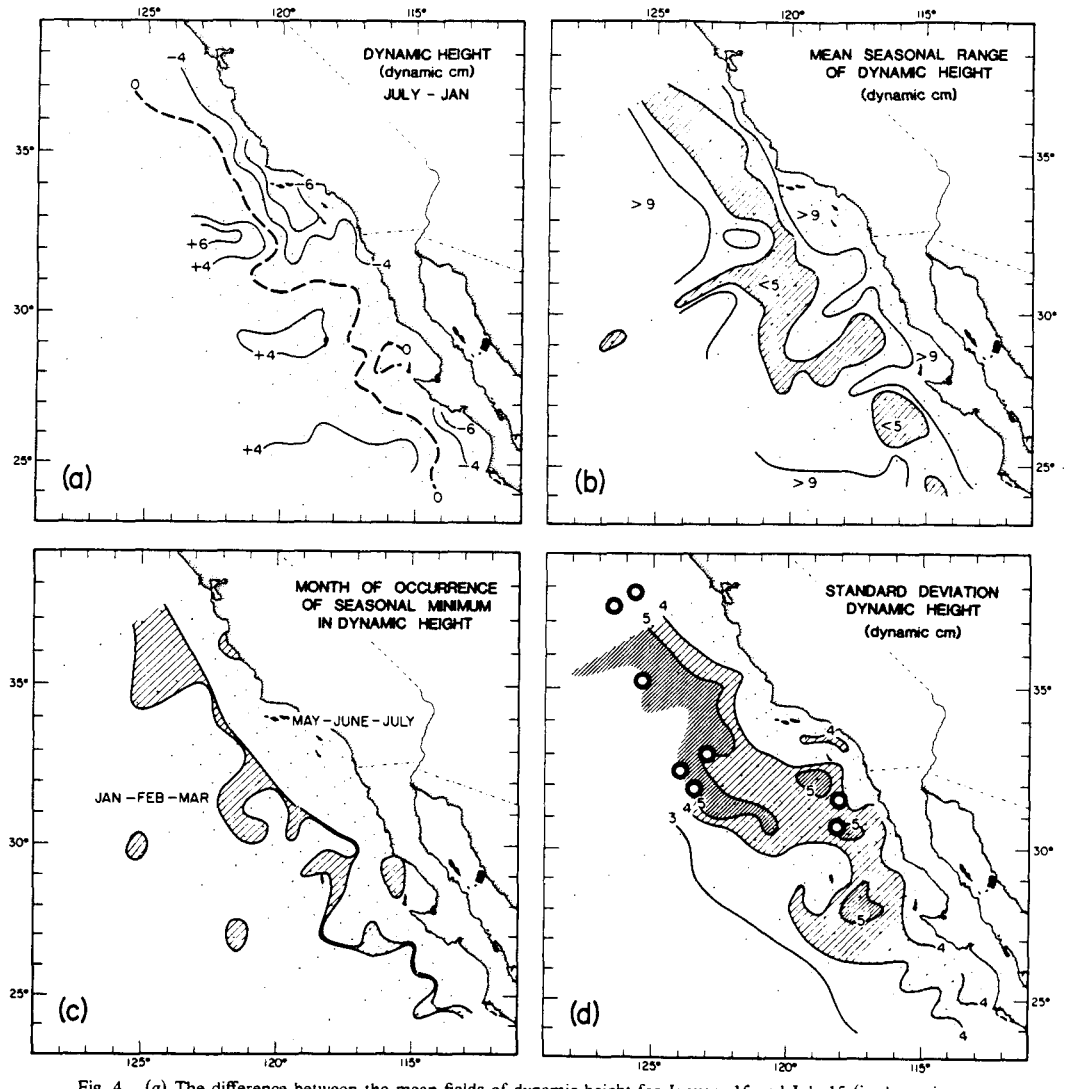

Fig. 4. (*a*) The difference between the mean fields of dynamic height for January 15 and July 15 (in dynamic centimeters). The zero line is shown dashed. (The characteristics depicted in Figures 4*a*–4*d* refer to dynamic height of the surface relative to 500 dbar. (*b*) The range of dynamic height derived from harmonic analysis (in dynamic centimeters). Range less than 5 dyn cm is hatched. (*c*) The months of occurrence of the seasonal minimum in dynamic height. Most months fall into two periods that are geographically separated. Those months that fell in neither period are separated by contours and hatched. (*d*) The standard deviation of dynamic height for the entire record of each station (i.e., seasonal variation was not removed). Standard deviation greater than 4 is hatched; standard deviation greater than 5 is densely hatched. The heavy circles give location of mesoscale eddies confirmed by independent studies.

ure 7). The IC, when it exists, is very narrow. Generally, where it exceeds 4 cm s^{-1}, it is defined solely by the inshore pair of stations along a given CalCOFI line. Typically, this inshore station spacing is about 30 to 50 km.

Seasonal variation in the strength and position of the high-velocity bands of these flows is more easily seen in plots of surface flow (0/500 dbar) perpendicular to each of the cardinal lines versus month (Plate 1). (Plate 1 can be found in the separate color section in this issue.) Such patterns of surface flow show strong regional differences. In one sense, each graph has some characteristics that are local in nature. The simplest of possible divisions consists of central California, southern California, and Baja California regions.

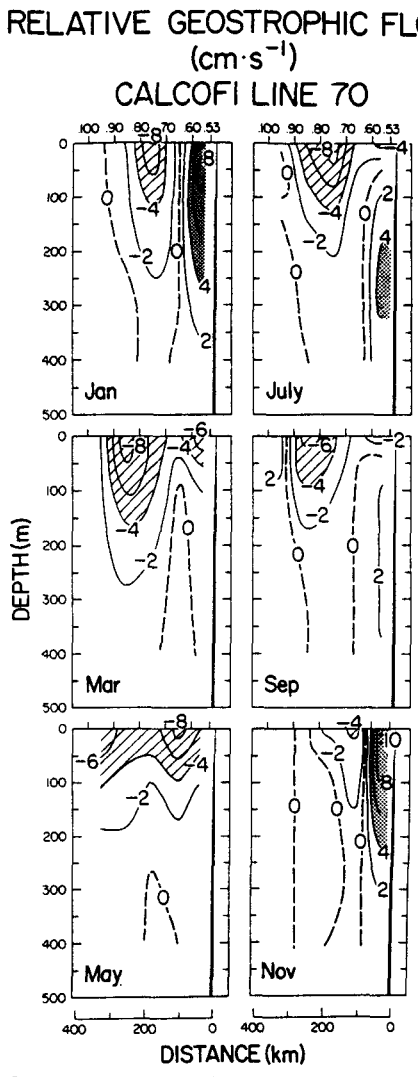

Fig. 5. Geostrophic velocity (in centimeters per second) relative to 500 dbar for odd months along CalCOFI line 70 (see Figure 1). Contour interval is 2 cm s^{-1}. Equatorward flow in excess of 4 cm s^{-1} is hatched. Poleward flow in excess of 4 cm s^{-1} is stippled.

Central California (lines 60, 70, and 80): The core of the surface equatorward flow is strongest approximately 200–300 km offshore with peak velocities occurring in the latter half of the year (Figure 5 and Plate 1). The inshore flow reverses direction seasonally; it is poleward in winter. The strongest inshore equatorward flow occurs in April–May at all three lines. Line 60 and line 80 both show semiannual variability in the nearshore region.

Southern California (line 90): There are two peaks in equatorward flow that are temporally and spatially distinct off southern California (Figure 6 and Plate 1). One occurs in midyear centered 70 km west of the offshore shallow bathymetric ridge (found at station 90.50, which is 173 km from shore). The second peak occurs in midwinter 180 km farther west. A line of zero flow lies above the bathymetric ridge. Shoreward of the bathymetric ridge, the poleward flow has two peaks: one in summer in the center of the Southern California Bight and another in late fall along the coast. The flow within the bight is mostly poleward. Equatorward flow does occur at the coast in August–September and very weakly so in March–April. The juxtaposition of the strong flow and counterflow of June–August is a space-time representation of the Southern California Eddy. Between these flows, Tanner Bank (~32.8°N, 119.2°W) is as shallow as 20 m.

Baja California (lines 100, 110, 120, and 130): The core of the equatorward surface flow is strongest along the coast; the maximum occurs in March and April (Figure 7 and Plate 1). There is a strong seasonal variability in the coastal equatorward flow. The seasonal reversal of this inshore flow, however, is very weak or nonexistent, with the exception of line 130 where there is a winter IC.

During March through May there is a tendency for all coastal flow in all three regions to be equatorward. North of the border this corresponds to a "spring transition" in the direction of inshore flow [*Huyer et al.*, 1979]. South of the border, inshore surface flow is equatorward most of the year. This equatorward flow peaks during the period of "spring transition" (Plate 1). A secondary peak occurs in equatorward flow 200 km offshore about June–July in three of the four station lines which define the Baja California region. There is strong semiannual variability inshore on line 130; a second strong equatorward flow occurs along the coast in August–September.

4.2.2. *Near-surface characteristics.* The mean distribution of salinity for July on the surface where σ_t = 25 (δ_t = 297 cl/ton = 297 × 10^{-5} ml/g) (Figure 8) demonstrates the well-defined tongue of low-salinity water which traces an offshore path roughly parallel to the coastline and oriented parallel to the mean geostrophic flow (Figure 2). A very similar salinity pattern is found in other months [*Lynn et al.*, 1982]. The σ_t = 25 surface intersects the sea surface near central California (marked by a bold line and shading in Figure 8). Elsewhere it lies in the upper gradient of the thermocline, about 60 m in the low-salinity core and 100 m near the western edge (see depth distribution of this density surface given by *Lynn et al* [1982, p. 395]). This pattern of salinity distribution does not differ in any fundamental way from the distribution of salinity at the sea surface. (Slightly lower salinity prevails where this surface coincides with the shallow minimum.) On this surface of constant density, however, the tongue of low salinity is also a tongue of low temperature because temperature and salinity uniquely define σ_t. Thus Figure 8 provides a clearer illustration of the transport of upper layer water characteristics than the sea surface temperature distribution would because sea surface temperature is markedly influenced by shallow wind-driven Ekman transport and surface heat exchange.

In the central California region the lowest salinity is found at the surface (line 60, Figure 9*a*). In the Baja California region the lowest salinity occurs in a well-defined subsurface (50 to 100 m) core [*Reid et al.*, 1958] which is

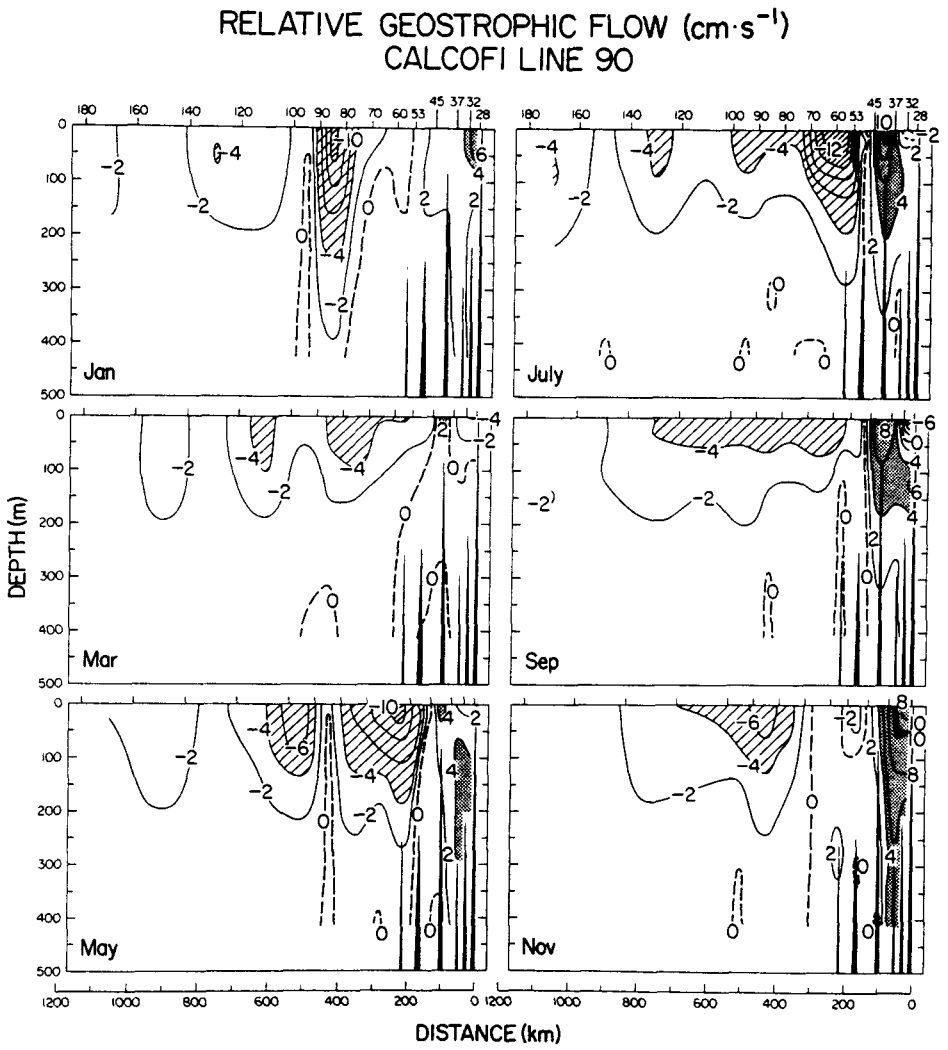

Fig. 6. Same as Figure 5 except for CalCOFI line 90.

close to the coast (line 110, Figure 9*c*). In the intermediate southern California region, the minimum salinity occurs at or very near the surface in July (line 90, Figure 9*b*). In fall there is a well-developed offshore subsurface salinity minimum (not shown). There is also a subsurface minimum inside the Southern California Bight [*Reid et al.*, 1964] caused by the recirculation of CC waters into the Southern California Bight. In summer the recirculation is intensified by the Southern California Eddy. The eddy is marked by the doming of higher-salinity waters at station 90.45 (Figure 9*b*).

In its equatorward path, the CC transports waters that have salinities as low as 33.7 to the vicinity of line 130 off southern Baja California (Figure 10). The subsurface salinity minimum has a larger lateral spread here than at line 110 and demonstrates a relatively large range of seasonal variation. In January, when there is a strong IC (Plate 1), waters with salinities below 33.8 are found offshore beyond the continental slope (hatched area in Figure 10). A strong equatorward flow coincides with the onshore return and surfacing of the salinity minimum layer in April and July. The October distribution is similar to that found in January, but unlike the January distribution, the surface inshore flow is strongly equatorward. The subsurface salinity minimum extends southward to 17°N [*Bennett*, 1963] and is carried westward in the North Equatorial Current [*Reid*, 1973; *Tsuchiya*, 1982].

In Figure 11 the lowest salinity found in the surface layer is plotted over the surface velocity graphs of Plate 1. For the most part, the (low-temperature) low-salinity core

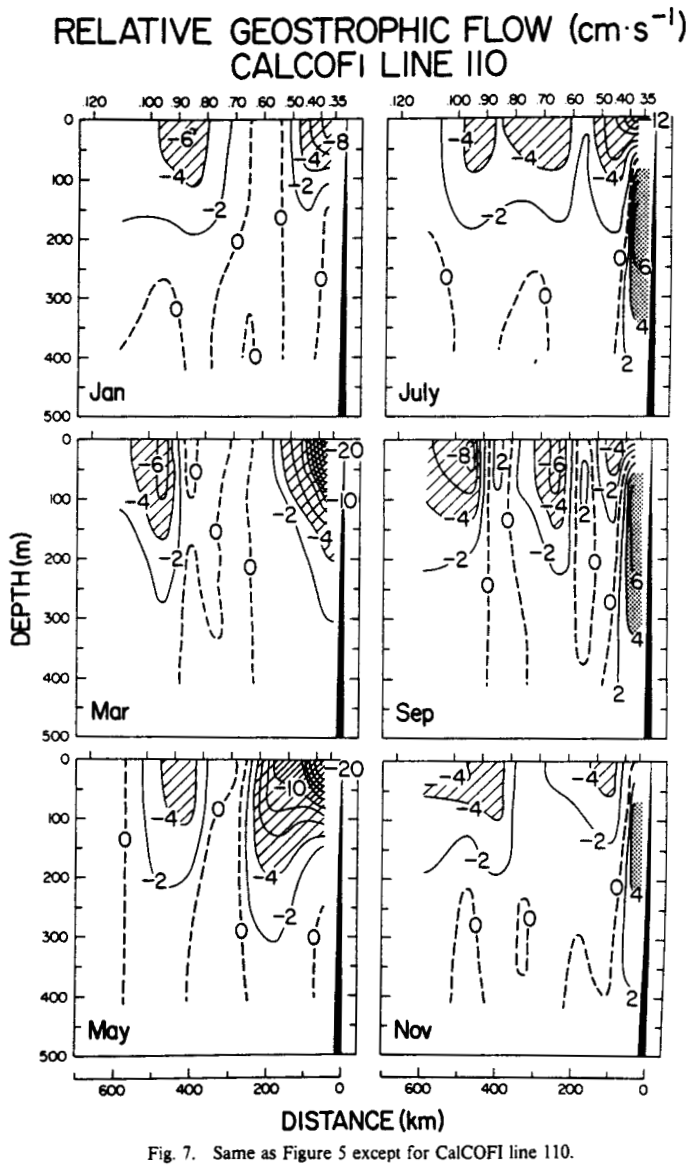

Fig. 7. Same as Figure 5 except for CalCOFI line 110.

falls in the regions of stronger equatorward flow. Despite the fact that salinity is measured at stations and velocity calculations are assigned between them, it is evident that the salinity minimum falls on the offshore side of the bands of high equatorward velocity. This suggests that there is greater infusion of salt into the low-salinity core from the higher-salinity coastal waters than from the offshore North Pacific Central waters. This pattern differs at line 90, where there are two strong flows and a double salinity minimum. The unique distribution of salinity at line 90 is caused by the upward displacement and mixing of deeper characteristics associated with the cyclonic circulation of the Southern California Eddy and the advection of low-salinity waters into the bight. This correspondence of strong flow and low salinity extends to depths of at least 100 m (Figures 5, 6, 7, and 9). Thus the low-salinity core is a good descriptor of the path of the California Current.

4.3. *Subsurface Flow and Characteristics*

4.3.1. *California Undercurrent.* The CU is a subsurface poleward flow. At 250 m, this poleward flow generally

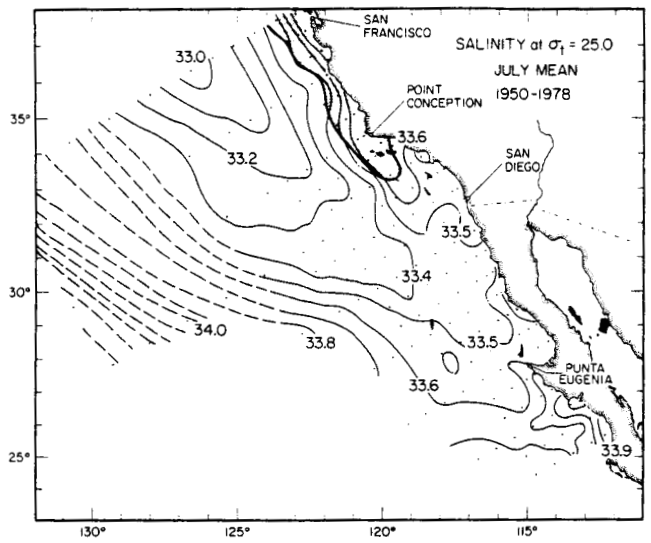

Fig. 8. Mean salinity on the surface where σ_t = 25.0 for July [from *Lynn et al.*, 1982]. The intersection of this density surface with the sea surface is indicated by a bold line. Where density is less (shown shaded), surface salinity is given. Contour interval is 0.1.

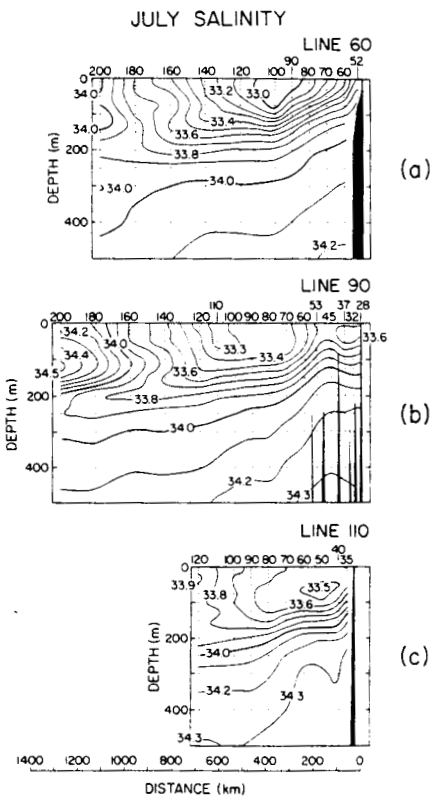

Fig. 9. Vertical sections of mean salinity for July along CalCOFI station lines 60, 90, and 110 [from *Lynn et al.*, 1982]. Contour interval is 0.1.

does not extend beyond 100 km from the coast (Figure 3); at greater depths it may extend to greater distances [e.g., *Hickey*, 1979]. Observations [*Reid*, 1962, 1963; *Wooster and Jones*, 1970] show that the CU has a high-velocity core along the continental slope. The seasonal cycle of the core of the CU is illustrated in Figure 12 (dashed lines), together with the surface flow above it

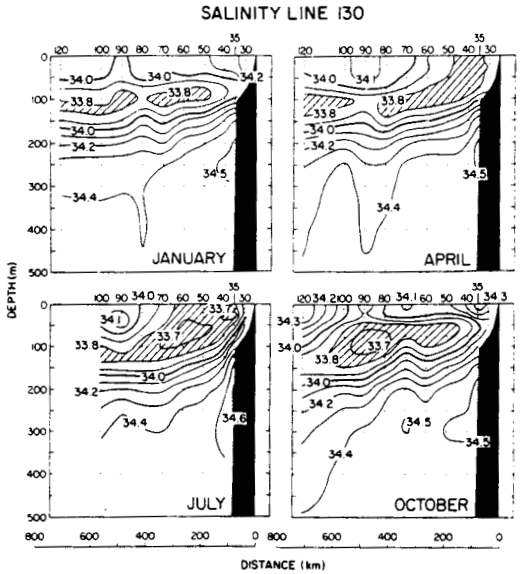

Fig. 10. Vertical sections of mean salinity along CalCOFI line 130 for four time periods [from *Lynn et al.*, 1982]. Salinities less than 33.8 are hatched. Contour interval is 0.1.

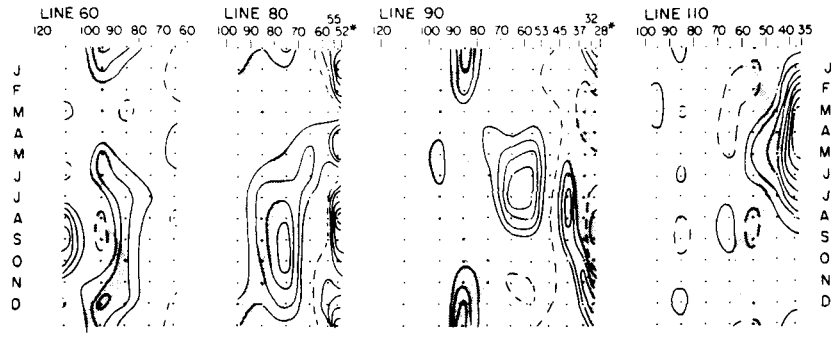

Fig. 11. The core of lowest-salinity California Current water (shaded) plotted on the velocity space-time graphs from Plate 1.

(solid lines). Relative geostrophic velocities were calculated using inshore pairs of stations, each reaching 500 m. Positive flow is poleward. At these station pairs the CU is defined as a subsurface maximum in poleward flow. Thus there is no CU when all flow is equatorward or when the maximum in poleward flow is at the surface or indistinguishable from the surface flow. The surface flow, when it is poleward, is labeled *IC for Inshore Countercurrent*; when it is equatorward, it is the CC.

In many places there is a tendency for flow to be poleward at some level year round. For the most part, this poleward flow is subsurface. At those places where there is a seasonal interruption, the interruption occurs for 2 or 3 months in spring (Figure 12). (Off southern Baja California there is also an interruption in fall (Figure 12*h*).) There is a strong semiannual variability in the CU off Central California (Figure 12*a*), off Point Conception (Figure 12*b*), and again within the Southern California Bight (Figure 12*d*) (see also *Hickey* [1979] and *Chelton* [1984]). This semiannual signal does not occur at the intermediate station line (Figure 12*c*) which lies seaward of Santa Rosa Island (~34°N, 120°W). This latter station pair is the only one in Figure 12 which is not adjacent to the coast. At many locations the CU diminishes in strength from January through March, and its core, defined by the subsurface maximum in poleward flow, is found at increasingly greater depths (Figure 13). From March through May at most coastal locations, the CU is either nonexistent or extremely weak (Figures 12 and 13). The correspondence of the weakening with the deepening of the CU suggests that the interruption of the CU in places could result from the assumption of zero flow at 500 dbar. After it reforms or increases in strength, in late spring and summer, it is found at increasingly shallower depths. In some instances the CU reaches a level where it is not discernible from the surface poleward current (e.g., Figure 12*a* and Figure 13*a*) (see also *Sverdrup et al.* [1942]). There are also long periods when the surface flow is equatorward, in opposition to the CU. In general, however, the geostrophic velocity at the sea surface is highly coherent with that at 250 m from central California to southern Baja California (Figure 12*a*–12*h*). *Chelton* [1984] observed this coherence north of the international border in relation to the upper 150 m. Further, he noted that an exception to this observation occurs at Point Conception (see Figure 12*b*). Over the outer continental slope the variability of the surface flow is annual, while that of the deeper flow is largely semiannual. A second exception is found at Punta Eugenia (Figure 12*g*). These two points are the major coastal capes in this study area. *Chelton* [1984] limited his study to the outer continental slope. An additional station, 80.52 (90 observations), falls over the inner slope at Point Conception. Although the sounding there is 220 m, the data record, for the purposes of time series analysis, is consistent to only 150 m. Geostrophic shear in the upper 150 m between stations 80.52 and 80.55 shows a very strong semiannual variability (Figure 12*i*). At Point Conception, therefore, the deeper outer slope flow is coherent with the surface flow over the inner slope. There is no inner slope CalCOFI station at Punta Eugenia with which to check for similar circumstances there. Because the amplitude of the variability in surface flow at Point Conception is much greater than that of the outer slope CU and because the surface flow lags the deeper flow by 1.5 months, shoreward extrapolation of the deeper flow produces a modest adjustment of the inshore surface geostrophic velocity (Figure 12*i*). This extrapolated velocity was used in Plate 1. There is a strong (11 cm s^{-1}) equatorward flow in spring and an equally strong (~13 cm^{-1}) poleward flow in August and again in January.

4.3.2. *Subsurface characteristics.* Distributions of characteristics on a surface of constant density that lies at middepths show the effects of transport at those depths. The 26.6 σ_t (δ_t = 145 cl/ton) surface lies between depths of 200 and 300 m along the coastal margin (Figure 14*a*). Peak velocity of the CU usually falls within or close to this range of depth during summer months and sometimes during winter (Figure 13). Distributions of salinity (and implicitly temperature) and oxygen on this density surface (Figures 14*b*, and 14*c*) illustrate the flow of the CU (Figure 12). Warm, saline, low-oxygen waters from subtropical latitudes are transported northward in a band along the coast. *Wooster and Jones* [1970] illustrated salinity in this manner for a July cruise. The extremes of high salinity, high temperature, and low oxygen found along the coastal margin are modified by lateral mixing with waters that are transported southward beyond 200 km offshore of California. The gradients of characteristics and isopleths of

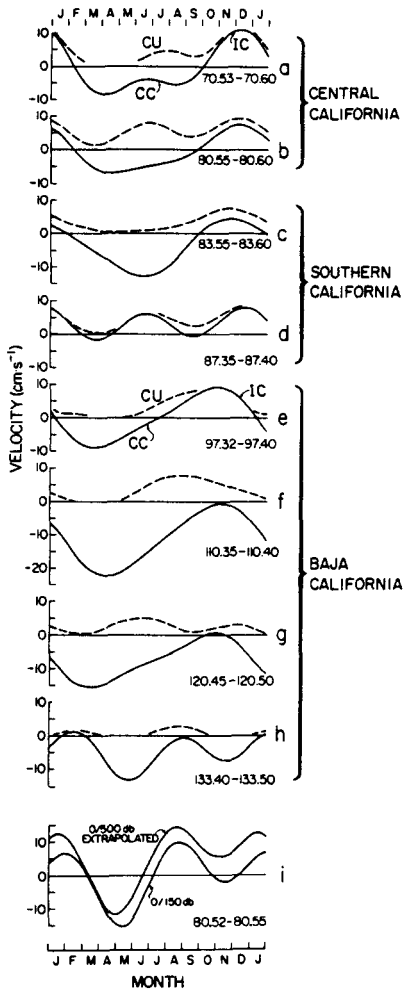

Fig. 12. (*a–h*) Relative geostrophic velocity (in centimeters per second) versus month for the California Current (CC) or surface Inshore Countercurrent (IC) (solid lines) and California Undercurrent (CU) (dashed lines) for station pairs from central California to southern Baja California that can be located in Figure 1. Each station pair lies adjacent to the continental shelf where there is at least 500 m of water. The CU is defined as a subsurface maximum in poleward flow; where the depth is less than 75 m it is not differentiated from the IC. (*i*) Two versions of relative geostrophic velocity at the surface over the inner continental slope near Point Conception (water depth 220 m). One uses a reference level of 150 dbar, and the other, based upon the shoreward extrapolation of deep shear, uses 500 dbar.

dynamic height suggest that in July this incursion of offshore waters is stronger off southern California and northern Baja California than elsewhere.

Depth, temperature, oxygen, and geostrophic velocity interpolated to levels where σ_t = 26.6 are plotted on a grid of distance along the cardinal lines versus time for an annual cycle. Contoured space-time graphs of these characteristics (Plate 2) demonstrate the relation between the seasonal flow of the CU and the characteristics it transports. (Plate 2 can be found in the separate color section in this issue.) This relation is particularly evident in the high-gradient region along the coastal margin. Along any given line there is a strong space-time coherence between characteristics. For example, the patterns for temperature and oxygen at line 110 (Plate 2*d*) are very similar. There is also a larger-scale space-time coherence both for a given characteristic and between characteristics from Point Sur (line 70) to Punta Eugenia (line 120) evidenced by the overall general similarity of most graphs in Plate 2. The flow of waters from the south along the coast carries the characteristics of higher temperature, higher salinity, and lower oxygen. Seasonally, the variation in strength of this flow results in a poleward extension or retreat of these extreme characteristics. The CU disappears at line 70 (Plate 2*a*) during March through May. Its disappearance slightly precedes the shallowest occurrence of the σ_t = 26.6 isopycnal (April through June) and the presence of the seasonally coolest and most oxygenated waters found at the coast (May and June). At line 80 (Plate 2*b*) there is a stronger semiannual signal in the CU than at line 70, as is evidenced in the corresponding temperature and oxygen distributions. Here the two strong pulses of the CU each precede both of the minima in oxygen and maxima in temperature. (The secondary temperature maximum is weak and is not revealed in the contours used in Plate 2*b*.) The effects of the summer development of the Southern California Eddy are evident at depth along line 90 in the vertical displacement of the density field (Plate 2*c*). The relative geostrophic velocity field shows that the influence of the eddy reaches 220 m. In fact, at σ_t = 26.6 the geostrophic velocity has essentially the same pattern, but at reduced values, as it has at the surface (Plate 1). The seasonal variation of nearshore characteristics within the Bight is not as strong as that observed off central California. Further south and inshore at line 110 (Plate 2*d*) there is a simple annual cycle; the CU disappears in spring 1 month before the minimum in

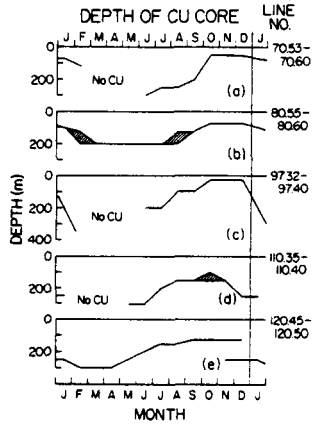

Fig. 13. Depth of the high-velocity core of the California Undercurrent versus month for some of the graphs of Figure 12.

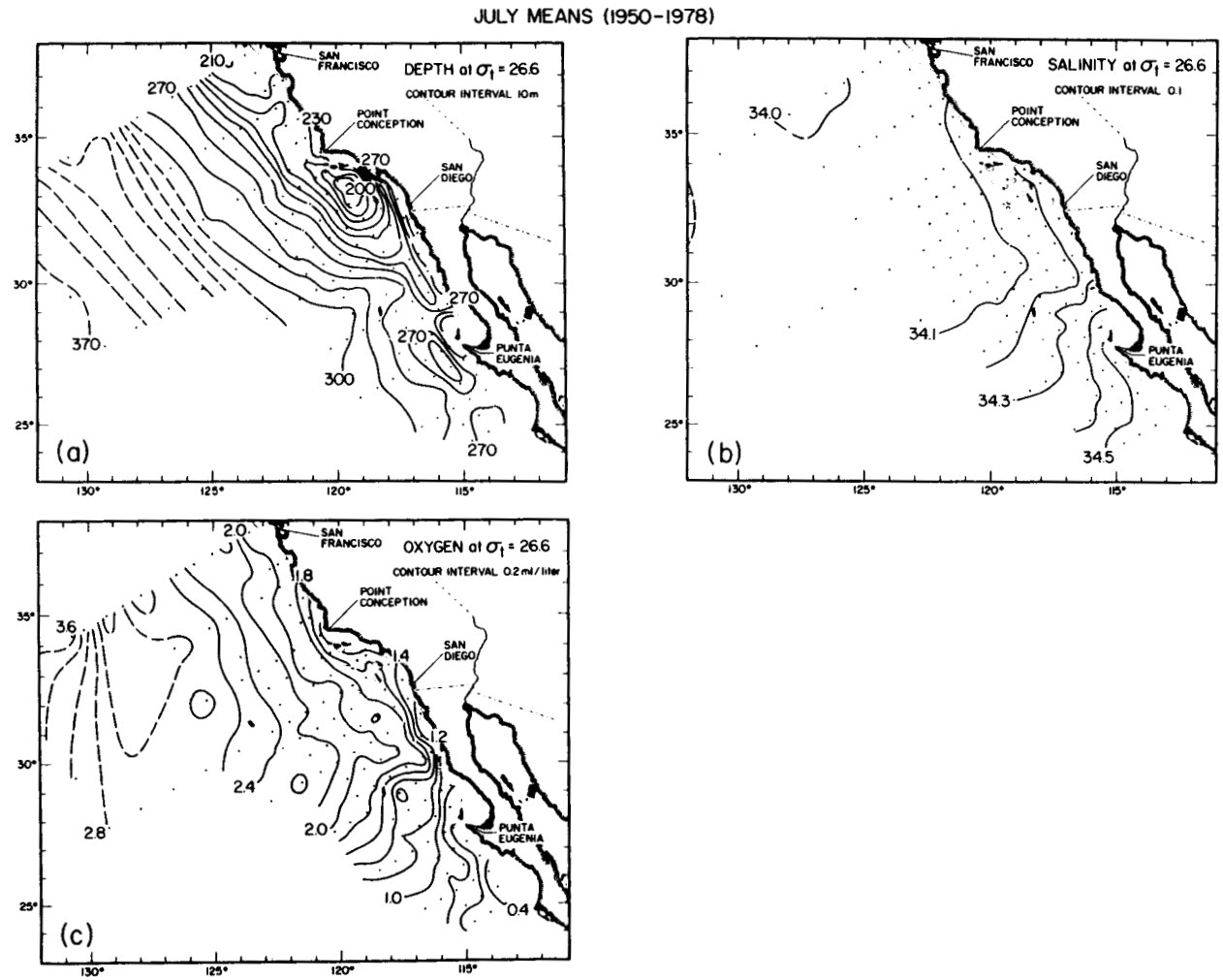

Fig. 14. (*a*) Mean depth (in meters) for July of the density surface σ_t = 26.6, (*b*) mean salinity, and (*c*) mean oxygen concentration (in milliliters per liter) for July on the σ_t = 26.6 surface (All from *Lynn et al.* [1982]).

temperature and maximum in oxygen. Distributions at line 120 (Plate 2*e*) show structure in coastal flow and characteristics similar to those on line 110. These distributions also show a response to the large-scale cyclonic eddy that strengthens in fall and whose center lies to the southeast of Punta Eugenia (Figure 3). The northern limb of this eddy carries warm, low-oxygen waters at least 550 km offshore during October through January (Plate 2*e*).

The foregoing description assumes that with the depth range of the σ_t = 26.6 surface the seasonal variation in advection dominates other processes affecting the seasonal variation of oxygen concentrations. The strong match of the seasonal patterns of oxygen to those of temperature suggest that to a first order, our assumption is correct.

5. DISCUSSION

5.1. *Dynamic Height*

The long-term, large-scale mean seasonal patterns in the surface (Figure 2) and subsurface (Figure 3) dynamic heights reflect the seasonal variability of the California Current, Inshore Countercurrent, and California Undercurrent. These patterns are similar to those presented by *Wyllie* [1966] and discussed by others [e.g., *Hickey*, 1979; *Chelton*, 1982; *Simpson*, 1984*b*].

The mean seasonal range of dynamic height (Figure 4*b*) and the months in which the seasonal minimum in dynamic height occurs (Figure 4*c*) define a coastal region, an offshore region, and a transition zone between them. In the offshore region the seasonal minimum occurs in winter, as would be expected from the effects of seasonal cooling. This is consistent with the large-scale open ocean distribution of dynamic height found in the eastern temperate North Pacific. There, seasonal changes in dynamic height are tied to the heating and cooling cycle [*Wyrtki*, 1975]; the minimum occurs in winter, the maximum in summer. Wyrtki finds that seasonal variations in dynamic height caused by changes in current patterns in the open ocean at temperate latitudes are generally much less than those caused by large-scale heating-cooling cycles. Shoreward of 200 km the opposite is true (Figures 4*b* and 4*c*). Here, the nearshore region has a seasonal variability in dynamic height that is dominated by processes other than the heating-cooling cycle [*Reid and Mantyla*, 1976]. In fact, seasonal variability in dynamic height in this domain is controlled by the seasonal occurrence of the IC and seasonal intensification of the CU (Figures 12 and 13). In the transition zone the month of occurrence of seasonal minimum in dynamic height has no pattern. It does not correspond to either periods of open ocean surface cooling or periods of inshore alterations in current flow (Figure 4*c*). It is unlikely that the ridge of high values in standard deviation of dynamic height (Figure 4*d*), coincident with the transition zone, would result simply from the combined influence of the neighboring regimes, each having a different physical forcing mechanism. Recurrent mesoscale eddies have been observed within this zone [e.g., *Bernstein et al.*, 1977; *Simpson et al.*, 1984]. Because the eddies have a large anomaly in dynamic height, the spatial and temporal variations of such eddies would readily boost the nonseasonal variation in dynamic height. Hence we suggest that the band of high standard deviation and of minimum seasonal range in dynamic height defines a zone in which there is a frequent occurrence of mesoscale eddies. Several independent sets of data support this interpretation. Maps for individual CalCOFI cruises show occurrences of enclosed contours and meanders within this transition zone that can be interpreted as eddies [*Wyllie*, 1966; *Burkov and Pavlova*, 1980] (see also the ongoing series of CalCOFI data reports). Some of these meanders are probably not eddies. There are, however, frequent occurrences of singular stations at which the dynamic height is significantly different than surrounding values; these singularities provide an unambiguous interpretation of an eddy. It is these latter realizations that contribute heavily to the formation of the band of high standard deviation in Figure 4*d*. Eddies whose signatures impress the long-term CalCOFI record must have length and persistence scales similar to those of the offshore eddies studied by *Simpson et al.* [1984]: 100 to 200 km and several weeks to several months. Other studies in the California Current system [*Reid et al*, 1963; *Bernstein et al.*, 1977; *Simpson et al.*, 1986; *Haury et al.*, 1986] also show mesoscale eddies that fall within this offshore band of high standard deviation in dynamic height. The positions of eddies from these studies and from eddies evident in published satellite-derived imagery [*Abbott and Zion*, 1985; *Lynn and Svejkovsky*, 1984] are plotted as circles in Figure 4*d*. All these data support the hypothesis of a transition zone populated with mesoscale eddies which lies between the coastal and open ocean flow regimes of the California Current system.

The interpretation of this zone of high standard deviation and low seasonality in dynamic height solely as an avenue of eddies is inappropriate. In general, the core of the CC lies within this band. The current core is defined by the relatively swifter meandering equatorward flow (Figure 2 and Plate 1) and the presence of the more extreme values of those measurands that characterize its source waters: low salinity and low temperature (Figure 8). Eddy-current field interactions are discussed in more detail in the following section.

5.2. *California Current and Inshore Countercurrent*

The California Current is an offshore, near-surface, permanent, equatorward flow. In the long-term average, this flow is slow, broad, and diffuse (Figure 2). The core of this flow is characterized by waters having relatively low temperature, low salinity (Figure 8), and high dissolved oxygen [e.g., *Lynn et al*, 1982]. Typical mean speeds are 4–12 cm s^{-1} in the upper 150 m of the water column (Figures 5, 6, and 7). Off central and southern California, the core of the CC generally occurs about 300–400 km offshore. Off Baja California, the core of the CC approaches within 200 km of the coast (Figure 2). The far offshore, semipermanent, high-salinity frontal structure, which is the southeastern extension of the Subarctic Frontal Zone (i.e., the California Front) is a good working definition of the western boundary of the CC proper. With this definition, the western boundary of the CC proper occurs about 900 km offshore.

The Inshore Countercurrent is a poleward flow which is confined primarily over the continental shelf and slope. Off central and southern California, it can extend as far as

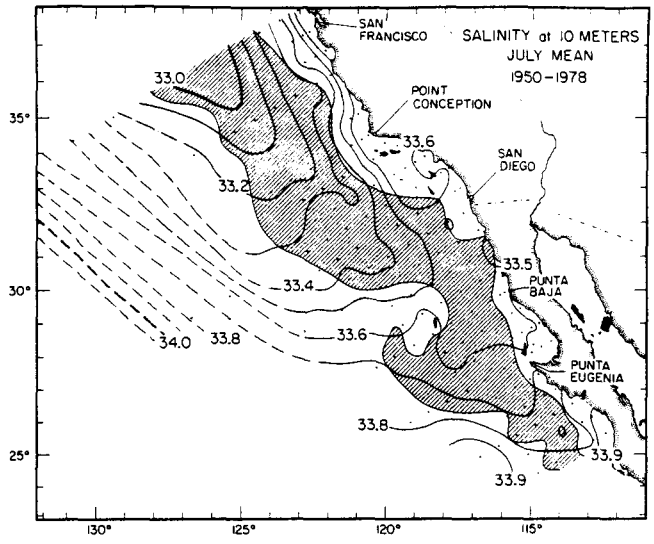

Fig. 15. Standard deviation of dynamic height ($>\pm 4$ dyn cm) from Figure 4*d* (shown hatched) plotted over on the long-term mean 10-m salinity for July [from *Lynn et al.*, 1982].

100 km offshore (Figure 2). It is confined to a more narrow coastal domain off Baja California, and in fact, off portions of northern Baja California there appears to be no poleward surface flow in the average (Figure 12) (unless it falls shoreward of our station pattern). There is a pronounced seasonal cycle in the appearance and strength of the IC (Figure 12 and Plate 1). Generally, the periods of maximum strength in the flow of the IC correspond with the periods of maximum strength in the flow of the California Undercurrent (Figures 12 and 13). In some months the poleward surface flow of the IC is spatially discontinuous (Figure 2), giving the appearance of inshore cyclonic eddies. During those periods when the inshore surface flow is equatorward, this flow is part of the overall flow of the California Current; along the coast the strongest equatorward flow generally occurs in spring.

"Spring transition" events are defined at nearshore locations by abrupt decreases in temperature and reductions in (or reversals of) the poleward flow over a considerable depth [*Huyer et al.*, 1979]. The CalCOFI data and the harmonic analysis used here cannot resolve the abrupt nature of the spring transition. We do note, however, the apparent simultaneity in springtime of either a reversal of the IC or an intensification of the CC along the coast from San Francisco to southern Baja California (~1500 km distance). This finding supports the conclusion by *Brink et al.* [1984] that the forcing mechanism for the spring transition occurs on a large spatial scale and does not seem to be associated with a coastally trapped wave.

In Figure 15 the standard deviation of dynamic height taken from Figure 4*d* is shown superimposed upon the long-term mean distribution of salinity at 10 m for July. This band of maximum in standard deviation, which defines the transition zone between coastal and oceanic regimes, generally lies within the region of offshore low-salinity core. The low-salinity core is itself a manifestation of the mean flow of the CC. Offshore mesoscale eddy activity significantly contributes to this band of maximum in standard deviation of dynamic height. There is also a contribution from the mean flow field. A region of enhanced gradient of dynamic height is found where the maximum flow occurs (e.g., Figure 2). Spatial variations, especially nonseasonal, in the position of the core of flow (i.e., meanders) create a maximum in standard deviation of dynamic height about the high-gradient region. These variations in the core of flow may themselves be associated with eddy activity. The combined distribution of salinity and standard deviation of dynamic height (Figure 15) supports the conclusion that there is a significant interaction between the CC and the offshore eddy field. The offshore eddy field in this band of maximum deviation is composed primarily of anticyclonic eddies [e.g., *Bernstein et al.*, 1977; *Burkov and Pavlova*, 1980; *Simpson et al.*, 1986]. Such eddies would tend to intensify the flow of the CC on the shoreward side of the eddy and diminish the flow of the CC on the westward side of the eddy. The effect of such an eddy-current interaction would be to produce a broadened core of low salinity by mixing and to displace the peak velocities of the CC shoreward of the low-salinity core (Figure 11).

Hickey [1979] discusses the mean flow of the CC based upon monthly arithmetic averages of dynamic height (e.g., her Figures 6 and 8). The averages she uses are from *Wyllie* [1966] and cover a period of 15 years (1950–1964). She hypothesizes that there are two distinct regions of strong southward flow separated by a region of reduced southward, or even northward, flow. Wyllie's maps of mean monthly dynamic topography, however, frequently lack sufficient numbers of observations (>3 per month) with which to calculate a meaningful average. This is

especially true north of San Francisco and at distances greater than 400 km from shore. The distributions of mean dynamic height we present (Figure 2) are based on arithmetic averages covering a period of 29 years (1950–1978). Evidence for multiple branches is far less clear in this updated version of the mean dynamic height field. Our interpretation of eddies (cyclonic or anticyclonic) imbedded in the CC core (Figures 4*d* and 15) would produce a strengthening of the equatorward flow on one side of the eddies and a weakening or reversal on the other side. Hence in a long-term average, this weakening of current in midstream could produce the appearance of branching of the CC. There is no evidence of branching in the distributions of water characteristics (Figure 8); lateral entrainment and subsequent mixing of inshore and offshore waters by the eddies [*Simpson*, 1984*c*; *Simpson et al.*, 1986; *Haury et al.*, 1986; *Liu et al.*, 1987] would, in a long-term average, destroy such evidence.

5.3. *California Undercurrent*

At depth, poleward flow occurs along the California–Baja California coast and, in most seasons, offshore to about 150 km. The highest speeds in the core of this flow are found along the continental slope. When and where the subsurface poleward flow reaches shallow levels ($\leq$ 50 m), it is barely distinguishable from the surface Inshore Countercurrent. This definition of the CU is consistent with direct current observations [e.g., *Reid*, 1962; *Wooster and Jones*, 1970] which show that the core of the CU is a narrow ribbon of high-speed ($\sim$30 cm s^{-1}) flow about 20 km in width and 300 m thick pressed against the continental slope.

The highest seasonal mean velocities of the CU are about 8 to 10 cm s^{-1} at various locations between San Francisco and Baja California (Figure 12). Poleward velocities exceeding 4 cm s^{-1} generally are confined to within 60 km of the coast off central and southern California (shaded in Figures 5 and 7). The CU also occurs along the continental slope in the Southern California Bight (Figure 6). Its appearance there, however, is complicated during summer and early fall by the strong poleward surface flow of the inshore limb of the Southern California Eddy. This inshore limb is centered 100 km offshore and recirculates the low-salinity waters of the offshore CC (Figure 11). Thus these recirculated waters are readily distinguishable from the more saline, subsurface poleward flowing waters of the CU.

The calculations of mean velocity (Figure 12) largely underestimate the high speeds of the narrow (20 km wide) core structure of the CU. They do, however, provide a general description of this current and its strong seasonal variation. Some of these seasonal graphs have a simple annual cycle; others have a strong semiannual cycle. The element in common among most of these graphs is the peak in velocity which occurs during late fall to early winter in the CU and/or IC, or a minimum in velocity where the surface flow is equatorward. This common element may be indicative of a larger-scale variation in driving forces than that which causes the more localized semiannual events evident within the bight (Figure 12*d*) and in the CU along central California (Figures 12*a* and 12*b*). In Figures 12*a* and 12*b* a second peak occurs in the CU-IC in summer. The summer peak of the CU and IC in the bight (Figure 12*d*) is apparently a response to the spin-up of the Southern California Eddy several tens of kilometers to the west. The summer peak in the CU at Point Conception and farther north may be a downstream (poleward) effect of this spin-up as evidenced by the northward decrease in the relative strength of this summer peak [see *Chelton*, 1984]. The very strong semiannual cycle of the IC off Point Conception (line 80) is evidenced in Plate 1, which uses an inshore station pair shallower than 500 m. The velocity graph for stations 83.55 and 83.60 off southern California (Figure 12*c*) shows a simple annual cycle. These stations are not located in the coastal zone; rather, they fall immediately seaward of the outer banks of the Southern California Bight (Figure 1*a*) and thus are unaffected by the summertime appearance of the Southern California Eddy.

Along southern Baja California the graphs of the annual cycle of velocity (Figures 12*g* and 12*h*) show considerably less coherence in their patterns. The large eddy off Punta Eugenia and complex patterns in the 200/500 dbar dynamic topography (Figures 2 and 3) demonstrate localized patterns in the seasonal cycles of the coastal flow. The large capes and partial embayments in the coastline and the proximity of the end of the Baja California peninsula contribute to these strong intraregional differences in patterns of flow.

We have chosen the σ_t = 26.6 (δ_t = 145 cl/ton) density surface to illustrate the distribution of deeper-water characteristics associated with the core of the CU because this density surface falls within a depth interval where the core is found. *Wooster and Jones* [1970] chose nearly the same surface (δ_t = 150 cl/ton) for the same reasons. The panels of Plate 2 show the seasonal variation in the distributions of these characteristics from central California to Baja California. Lowest dissolved oxygen concentration is centered over the continental slope throughout this domain. The domain of low-oxygen water also is a domain of warm, saline water. (Warm waters imply saline waters on a surface of constant density.) These extremes of low oxygen, high temperature, and high salinity occur within the region of maximum subsurface poleward flow.

The seasonal variation in the extremes of these characteristics also coincides temporally with the seasonal variation in the strength of the CU core. This seasonal variation is particularly evident in the high-gradient regions along the coastal margin. Here, the seasonal increase in transport of waters from the south along the coast causes extremes in the high temperature and salinity and low oxygen; the seasonal slackening in transport of these waters results in the lessening of the extremes. There is no CU at line 70 (Plate 2*a*) during March through May. Its disappearance slightly precedes the shallowest occurrence of σ_t = 26.6 (April through June) and the presence of the coolest and most oxygenated waters at the coast (May and June). May and June are also the months of strongest upwelling [*Bakun*, 1975]. At line 80 (Plate 2*b*) there is a stronger semiannual signal to the CU than at line 70, as is evidenced in the corresponding temperature and oxygen distributions. Here the two strong pulses of the CU each precede both of the minima in oxygen and maxima in temperature. (The secondary temperature maximum is weak and is not revealed in the contours used in Plate 2*b*.) These contour patterns also demonstrate the strong large-scale interrelationship between corresponding fields. For example, the tempera-

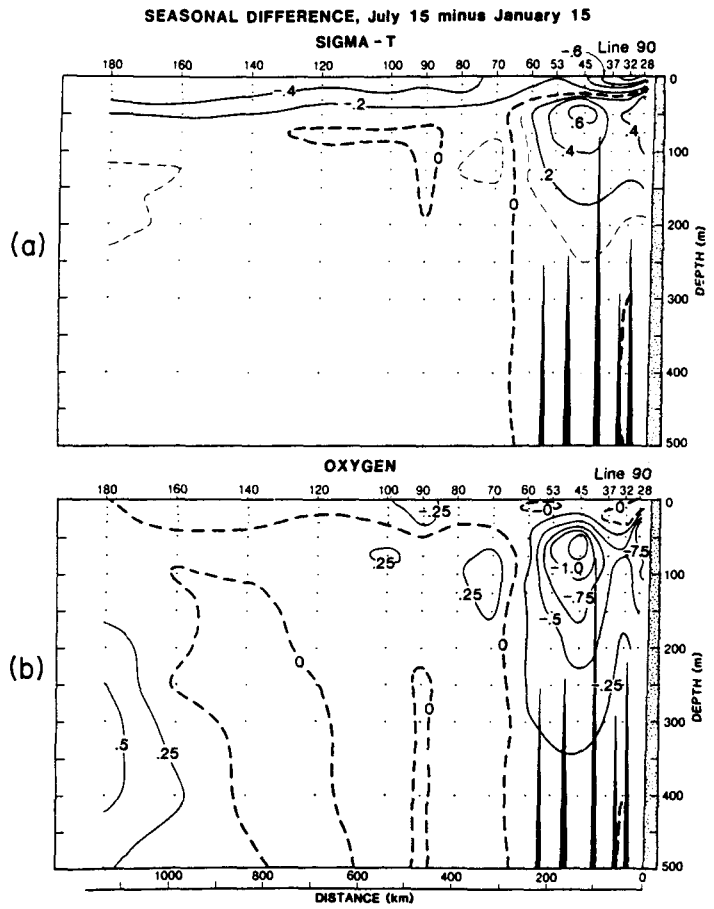

Fig. 16. (*a*) Vertical section of the difference between mean fields of σ_t along line 90 for January 15 and July 15. (*b*) The corresponding plot for oxygen difference.

ture (salinity) and oxygen patterns are nearly identical over the entire CalCOFI region.

There is usually a peak in the flow of the CU during late fall or in the IC where and when the CU shoals and becomes a surface current (Figure 13). At most locations the peak velocities of the IC or, where appropriate, the minimum values in the inshore CC, coincide with this strengthening and shoaling of the CU (Figures 12 and 13). This coincidence suggests that the IC is a surfacing of the CU. Additionally, the period of maximum in the IC flow also corresponds to the period of reduced surface wind stress [*Nelson*, 1977]. During this same period the distribution of inshore salinity on the deep σ_t = 26.6 density surface (Plate 2) and the shallower σ_t = 25.8 surface [*Lynn et al.*, 1982] is higher than during spring and summer. Likewise, during this period the oxygen on these same density surfaces is lower. After January the CU decreases in strength and deepens, and by March it disappears in many locations, at least with respect to the assumption of zero flow at 500 dbar. (This assumption requires testing in the vicinity of the continental slope.) This deepening of the CU coincides with the return of persistent northwesterly winds. Thus the CU, which likely has a nonlocal density-driven component of forcing, surfaces and becomes the IC during periods of minimum surface wind forcing (October to February). During periods of maximum wind forcing (March to August), inshore surface equatorward flow overlies the CU.

5.4. *Seasonal Differences: Vertical Sections*

Seasonal variability in the strength of baroclinic flow changes the distribution of characteristics in the water column in two ways: (1) through the local vertical readjustment of the water column to a time-varying baroclinic field and (2) through time-varying lateral transport of nonlocal waters with different characteristics (i.e., with lateral gradients in T, S, and O_2). A vertical section of the difference in σ_t between mid-January and mid-July for line 90 (Figure 16) coupled with characteristic curves (Figure 17) illustrates this point. The decrease of σ_t in the surface layer (upper 25 to 50 m) from January to July

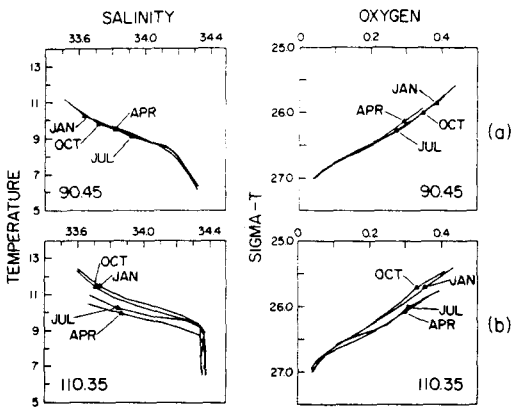

Fig. 17. Temperature versus salinity and oxygen versus σ_t for stations 90.45 and 110.35. Plots are given for January, April, July, and October. Values are plotted for depths of 75–500 m. The values at 100 m are marked by solid triangles for each month.

reflects the local seasonal warming. (The corresponding increase in surface temperature is 1.2° to 4.8°C.) Between the coast and station 70 and below 30 m there is an increase of σ_t over this period that reflects the change in the density field associated with the spin-up of the Southern California Eddy. The doming in the density field is also seen as a large negative anomaly in oxygen (Figure 16*b*) and negative and positive anomalies in the fields of temperature and salinity, respectively (not shown). That the local vertical readjustment to a seasonally varying geostrophic velocity field explains the greater part of the seasonal change in characteristics is evident in station plots (for 75 m and deeper) of temperature versus salinity and oxygen versus density (Figure 17*a*). The temperature versus salinity and oxygen versus σ_t curves for station 90.45 are very nearly seasonally invariant. The indications of the 100-m level on these four "seasonal" plots, however, demonstrate that there is a strong seasonal variation at this level. It is the local vertical readjustment of the water column to the seasonally varying flow field that produces changes at this and other levels. Station 90.45 lies near the center of the Southern California Eddy.

At other stations there is a significant seasonal change in water mass characteristics that can account for a sizable portion of the overall variation at depth. Many of these stations are located along the coastal margin. As an example, at station 110.35 (Figure 17*b*), the seasonal range of differences in T-S and O_2-σ_t curves is of the same order as the range for the sample depth given in the figure. This station is found close against the continental slope and in a region where there is a strong and varying surface (Plate 1) and subsurface flow (Figure 12). The northward penetration of warm, saline, low-oxygen water along the coastal margin is seen to extend and withdraw in the series of distributions on the 26.6-σ_t surface (Plate 2).

The time of occurrence of the maximum in σ_t versus depth and distance offshore from central to Baja California falls into simple patterns (Figure 18). In the surface layer the maximum occurs in late winter as a consequence of seasonal cooling. There is abrupt change below the surface layer in the offshore region, shown by a bold contour, where the maximum occurs in late summer and fall as a result of the vertical adjustment of the water column to a seasonal relaxation of the geostrophic flow of the CC. A vertical bold contour divides the offshore and nearshore zones. In the nearshore zone the maximum occurs in April–May, a period in which there is a spring transition characterized by a decrease or reversal of coastal poleward flow or a strong surge of equatorward flow. The stations nearest the vertical bold contours in Figure 18 (e.g., 70.60) often have a strong semiannual variation in the phasing of σ_t because of the interplay of the nearshore and offshore events. This narrow zone where the density field pivots on a horizontal axis coincides with the transition zone between coastal and oceanic regimes defined by the field of dynamic height (Figure 4). The phasing found at station 110.120 (Figure 18) appears to be a singularity (see also Figure 4*c*) and may be the result of inadequate sampling (15 observations).

The opposite phase of this σ_t cycle is not as coherent; the minimum in σ_t does not form such a simple set of patterns. A decrease in σ_t occurs in the surface layer in late summer as a result of seasonal warming and also at depth in winter along the coast as a result of the local adjustment of σ_t to the seasonally varying poleward CU flow. The peak velocities of the CU, however, occur over an extended period, and in some regions there are two

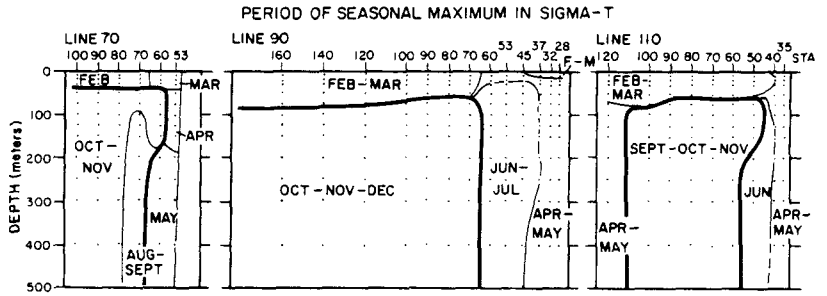

Fig. 18. Vertical sections showing the months of the seasonal maximum in σ_t for CalCOFI lines 70, 90, and 110. The heavy contour denotes a temporal discontinuity.

such periods. Thus the phasing of the seasonal minimum in σ_t is less well structured.

5.5. *Regional Differences*

The sets of characteristics at each of the cardinal lines often reveal regional peculiarities. For instance, line 70 is well situated to show events typical of the very nearly straight coastline of central California along which there are frequent northwest winds parallel to the coast and strong upwelling. Line 80, 220 km to the south, lies off a point of land where there is a major reorientation of the coastline. A coastal undercurrent and/or surface counterflow about this point intermittently disrupts the local effects of upwelling, and hence the patterns of temperature and oxygen differ from the regions to the north. Line 90 bisects the Southern California Bight and its offshore banks. These bathymetric features create their own signature in the distributions. Line 100 lies in a region where either there is an onshore limb of the Southern California Eddy or an intensified CC pressed against the coast. The record at line 110 provides a more consistent picture of the intensified flow along the coast of northern Baja California. Line 120 lies slightly northeast of Punta Eugenia, the most prominent projection of land in the study area. This station line lies in the northern limb of a large cyclonic eddy that intensifies seasonally. Line 130, which lies off a large bight, is rather lightly sampled for the complex frontal events evident there. Cardinal lines 70, 90, and 110 are the most suitable as representative examples of large regions of the generalized southeast-northwest flow patterns; flow is mostly perpendicular to these lines.

6. CONCLUSIONS

The seasonal variation of the physical characteristics and large-scale current patterns of the California Current system are examined using harmonic analysis applied to the 1950–1978 CalCOFI data set. The study covered the California Current system from the coast to approximately 1000 km offshore and from San Francisco to Baja California. The major conclusions of this study are as follows:

1. There are three domains; oceanic, coastal, and an intervening transition zone, defined by the amplitude and phasing of the seasonal variation of the dynamic height and by the standard deviation of the overall record of dynamic height. Dynamic height in the oceanic domain is controlled by large-scale air-sea interaction processes and large-scale dynamics. In the coastal domain it is dominated by alterations in the inshore surface and subsurface current structure. In the transition zone, variations of dynamic height are dominated by nonseasonal events: offshore mesoscale eddies and meanders in the high-speed core of the California Current.

2. The California Current is primarily an offshore, near-surface (0–300 m) equatorward flow whose core is characterized by low salinities and low temperatures. Off central and southern California the core of the CC usually occurs 300 to 400 km offshore, and off Baja California it occurs within 200 km of the coast.

3. The region of the low-salinity, high geostrophic velocity core also corresponds to the eddy-dominated transition zone.

4. Distribution of characteristics shows that there is a strong interaction between the core of the CC and the mesoscale eddy field.

5. The seasonal cycle of flow within the California Current system is characterized by the seasonal appearance of the Inshore Countercurrent and the Southern California Eddy and by the intensification of the California Undercurrent. Evidence suggests that the fall–winter appearance of the IC is associated with the shoaling of the CU.

6. The strong semiannual oscillation of the IC and CU in the Southern California Bight and regions farther north may be related to the seasonal development of the Southern California Eddy.

7. Below the surface layer (or upper thermocline) the seasonal variation of water mass characteristics is related to both the vertical adjustment of the water column to seasonally varying geostrophic currents and to varying transport of waters from different sources.

8. At depths of the CU core there is a seasonal variation in the water mass characteristics that is associated with the variation in the strength of the flow.

9. There is a strong coherent pattern in phasing of σ_t with depth and distance offshore. The transition zone, as defined by the statistics of the dynamic height field, has vertical extent as evidenced by the lateral discontinuity in the pattern of σ_t phasing.

10. The vertical discontinuity in σ_t phasing shows that below about 100 m, seasonal variation in density is controlled largely by dynamic processes. Above 100 m, however, thermodynamic processes also are important.

Acknowledgments. This study would not have been possible without the extensive efforts that many dedicated individuals have contributed to the long-standing CalCOFI program. The large archive of physical oceanographic data is a data set that is unique in so many ways, especially in its high level of quality and its spatial and temporal coverage. We wish to express our thanks to L. Eber for providing the data file and assisting in its manipulation, to S. McBride for typing the many versions of our manuscript, and to N. Hulbirt and G. Tapper for drafting the figures. Partial financial support was provided to J.J.S. by the Marine Life Research Group of the Scripps Institution of Oceanography, the California Space Institute, and the Office of Naval Research under contract N00014-86-K-0752.

REFERENCES

Abbott, M. R., and P. M. Zion, Satellite observations of phytoplankton variability during an upwelling event, *Cont. Shelf Res.*, *4*, 661–680, 1985.

Bakun, A., Daily and weekly upwelling indices, West coast of North America, 1967–73, *NOAA Tech. Rep., NMFS SSRF 693*, 114 pp., 1975.

Bennett, E. B., An oceanographic atlas of the eastern tropical Pacific Ocean, based on data from EASTROPIC expedition, October–December 1955, *Inter Am. Trop. Tuna Comm. Bull.*, *8-2*, 165 pp., 1963.

Bernstein, R. L., L. Breaker, and R. H. Whritner, California Current eddy formation: Ship, air, and satellite results, *Science*, *195*, 353–359, 1977.

Brink, K. H., D. W. Stuart, and J. C. Van Leer, Observations of the coastal upwelling region near 34°30'N off California: Spring 1981, *J. Phys. Oceanogr.*, *14*, 378–391, 1984.

Burkov, V. A., and Yu. V. Pavlova, Description of the eddy field of the California Current, *Oceanology*, Engl. Transl., *20(3)*, 272–278, 1980.

Chelton, D. B., Large-scale response of the California Current to forcing by the wind stress curl, *CalCOFI Rep. 23*, pp. 130–148, Calif. Coop. Oceanic Fish. Invest., La Jolla, 1982.

Chelton, D. B., Seasonal variability of alongshore geostrophic velocity off central California, *J. Geophys. Res., 89*, 3473–3486, 1984.

Davis, R. E., Drifter observations of coastal surface currents during CODE: The method and descriptive view, *J. Geophys. Res., 90*, 4741–4755, 1985.

Eber, L. E., and N. Wiley, Revised update and retrieval system for the CalCOFI oceanographic data file, *NOAA Tech. Memo., NOAA-TM-NMFS-SWFC-24*, 69 pp., 1982.

Godfrey, J. S., and K. R. Ridgway, The large-scale environment of the poleward-flowing Leeuwin Current, Western Australia: Longshore steric height gradients, wind stresses and geostrophic flow, *J. Phys. Oceanogr., 15*, 481–495, 1985.

Haury, L. R., J. J. Simpson, J. Peláez, C. J. Koblinsky, and D. Wiesenhahn, Biological consequences of a recurrent eddy off Point Conception, California, *J. Geophys. Res., 91*, 12,937–12,956, 1986.

Hickey, B. M., The California Current system—hypotheses and facts, *Prog. Oceanogr., 8*, 191–279, 1979.

Huyer, A., E. J. C. Sobey, and R. L. Smith, The spring transition in currents over the Oregon continental shelf, *J. Geophys. Res., 84*, 6995–7011, 1979.

Liu, H. T., J. J. Simpson, and J. C. Schedvin, Preliminary laboratory study of the lateral entrainment of non-local waters by a subsurface mesoscale eddy, *Exp. Fluids*, in press, 1987.

Lynn, R. J., Seasonal variation of temperature and salinity at 10 m in the California Current, *CalCOFI Rep. 11*, pp. 157–186, Calif. Coop. Oceanic Fish. Invest., La Jolla, 1967.

Lynn, R. J., The subarctic and northern subtropical fronts in the eastern North Pacific Ocean in spring, *J. Phys. Oceanogr., 16*, 209–222, 1986.

Lynn, R. J., and J. Svejkovsky, Remotely sensed sea surface temperature variability off California during a "Santa Ana" clearing, *J. Geophys. Res., 89*, 8151–8162, 1984.

Lynn, R. J., K. A. Bliss, and L. E. Eber, Vertical and horizontal distributions of seasonal mean temperature, salinity, sigma-*t*, stability, dynamic height, oxygen, and oxygen saturation in the California Current, 1950–1978, *CalCOFI Atlas 30*, 513 pp., State of Calif. Mar. Res. Comm., La Jolla, 1982.

Montgomery, R. B., Transport of the Florida Current off Habana, *J. Mar. Res., 4*, 198–219, 1941.

Nelson, C. S., Wind stress and wind stress curl over the California Current, *NOAA Tech. Rep., NMFS SSRF-714*, 89 pp., 1977.

NORPAC Committee, *Oceanic Observations of the Pacific, The NORPAC Atlas*, 11 pp., 123 plates, Univ. of Calif. Press, Berkeley, 1960.

Pickard, G. L., *Descriptive Physical Oceanography*, 214 pp., Pergamon, New York, 1964.

Reid, J. L., Jr., Measurements of the California Countercurrent at a depth of 250 km, *J. Mar. Res., 20*, 134–137, 1962.

Reid, J. L., Jr., Measurements of the California Countercurrent off Baja California, *J. Geophys. Res., 68*, 4819–4822, 1963.

Reid, J. L., The shallow salinity minimum of the Pacific Ocean, *Deep Sea Res., 20*, 51–68, 1973.

Reid, J. L., and A. W. Mantyla, The effects of the geostrophic flow upon coastal sea elevations in the northern North Pacific Ocean, *J. Geophys. Res., 81*, 3100–3110, 1976.

Reid, J. L., Jr., and R. A. Schwartzlose, Direct measurements of the Davidson Current off Central California, *J. Geophys. Res., 67*, 2491–2497, 1962.

Reid, J. L., Jr., G. I. Roden, and J. G. Wyllie, Studies of the California Current system, *CalCOFI Rep. 6*, pp. 27–56, Calif. Coop. Oceanic Fish. Invest., La Jolla, 1958.

Reid, J. L., R. A. Schwartzlose, and D. M. Brown, Direct measurements of a small surface eddy off northern Baja California, *J. Mar. Res., 21*, 205–218, 1963.

Reid, J. L., Jr., E. Coughran, and C. Worral, Detailed measurements of a shallow salinity minimum, *J. Geophys. Res., 69*, 4767–4771, 1964.

Saur, J. F. T., Surface salinity and temperature on the San Francisco–Honolulu Route, June 1966–December 1970 and January 1972–December 1975, *J. Phys. Oceanogr., 10*, 1669–1680, 1980.

Simpson, J. J., El Niño–induced onshore transport in the California Current during 1982–83, *Geophys. Res. Lett., 11*, 233–236, 1984*a*.

Simpson, J. J., A simple model of the 1982–83 Californian "El Niño," *Geophys. Res. Lett., 11*, 237–240, 1984*b*.

Simpson, J. J., An offshore eddy in the California Current system, III, Chemical structure, *Prog. Oceanogr., 13*, 71–93, 1984*c*.

Simpson, J. J., T. D. Dickey, and C. J. Koblinsky, An offshore eddy in the California Current system, I, Interior dynamics, *Prog. Oceanogr., 13*, 5–49, 1984.

Simpson, J. J., C. J. Koblinsky, J. Peláez, L. R. Haury, and D. Wiesenhahn, Temperature–plant pigment–optical relations in a recurrent offshore mesoscale eddy near Point Conception, California, *J. Geophys. Res., 91*, 12,919–12,936, 1986.

Sverdrup, H., On the process of upwelling, *J. Mar. Res., 1*, 155–164, 1938.

Sverdrup, H. U., M. W. Johnson, and R. H. Fleming, *The Oceans, Their Physics, Chemistry, and General Biology*, 1087 pp., Prentice-Hall, Englewood Cliffs, N. J., 1942.

Sverdrup, H. U., and R. H. Fleming, The waters off southern California March to July 1937, *Bull. of the Scripps Inst. of Oceanogr. of the Univ. of Calif.*, La Jolla, *4*, pp. 261–378, 1941.

Tsuchiya, M., On the Pacific upper-water circulation, *J. Mar. Res., 40*, Suppl., 777–799, 1982.

Wooster, W. S., and J. H. Jones, California Undercurrent off northern Baja California, *J. Mar. Res., 28*, 235–250, 1970.

Wyllie, J. G., Geostrophic flow of the California Current at the surface and at 200 m, *CalCOFI Atlas 14*, 12 pp., 288 charts, State of Calif. Mar. Res. Comm., La Jolla, 1966.

Wyrtki, K., Fluctuations of the dynamic topography in the Pacific Ocean, *J. Phys. Oceanogr., 5*, 450–459, 1975.

R. J. Lynn, Southwest Fisheries Center, National Marine Fisheries Service, P.O. Box 271, La Jolla, CA 92038.

J. J. Simpson, Scripps Institution of Oceanography, La Jolla, CA 92093.

(Received February 14, 1987;
accepted April 6, 1987.)

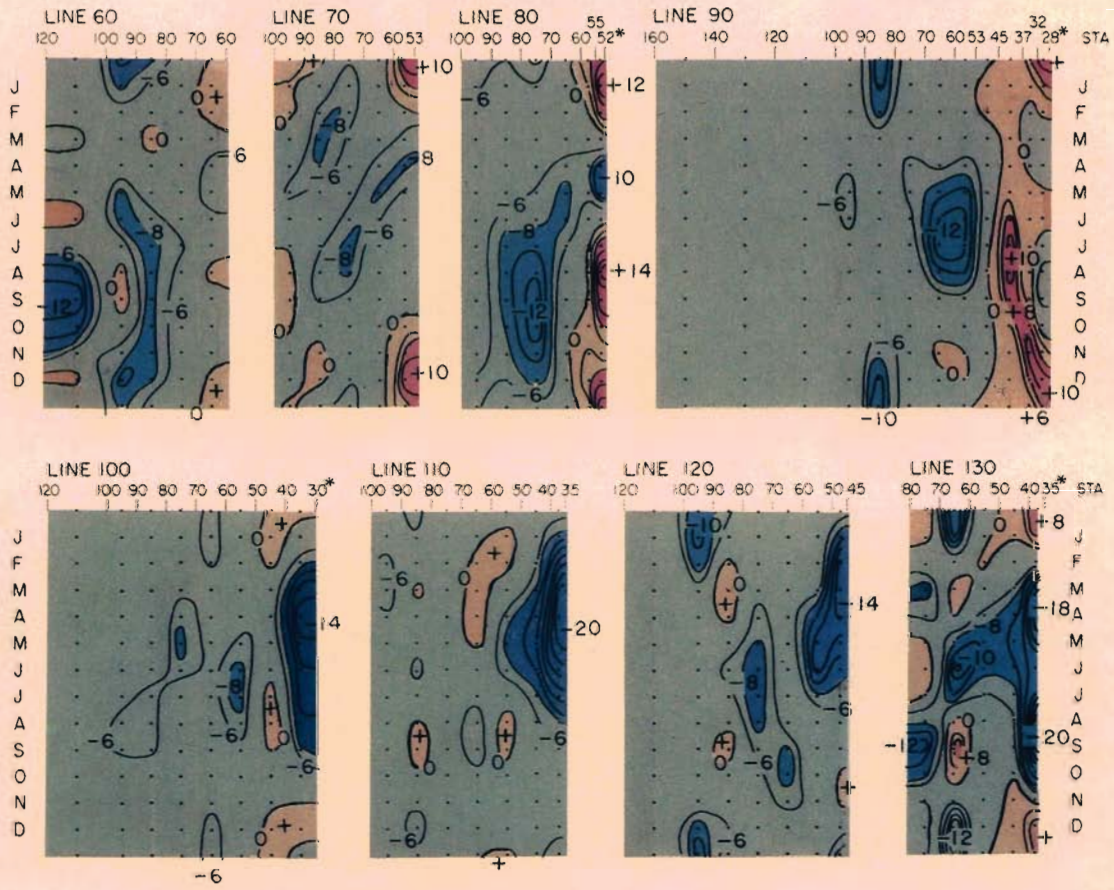

Plate 1 [*Lynn and Simpson*]. Space-time graphs of mean seasonal surface geostrophic velocity perpendicular to cardinal lines for an annual cycle. The CalCOFI station numbers are identified at the top of each graph. The starred stations required extrapolation of the slope in the offshore dynamic height field below 150 m for station 80.52, below 200 m for station 90.28, and below 300 m for stations 100.30 and 130.35. Velocity greater than 6 cm s^{-1} is contoured at intervals of 2 cm s^{-1}. Equatorward flow is colored blue; poleward flow is pink. Color intensity increases at 8 cm s^{-1}.

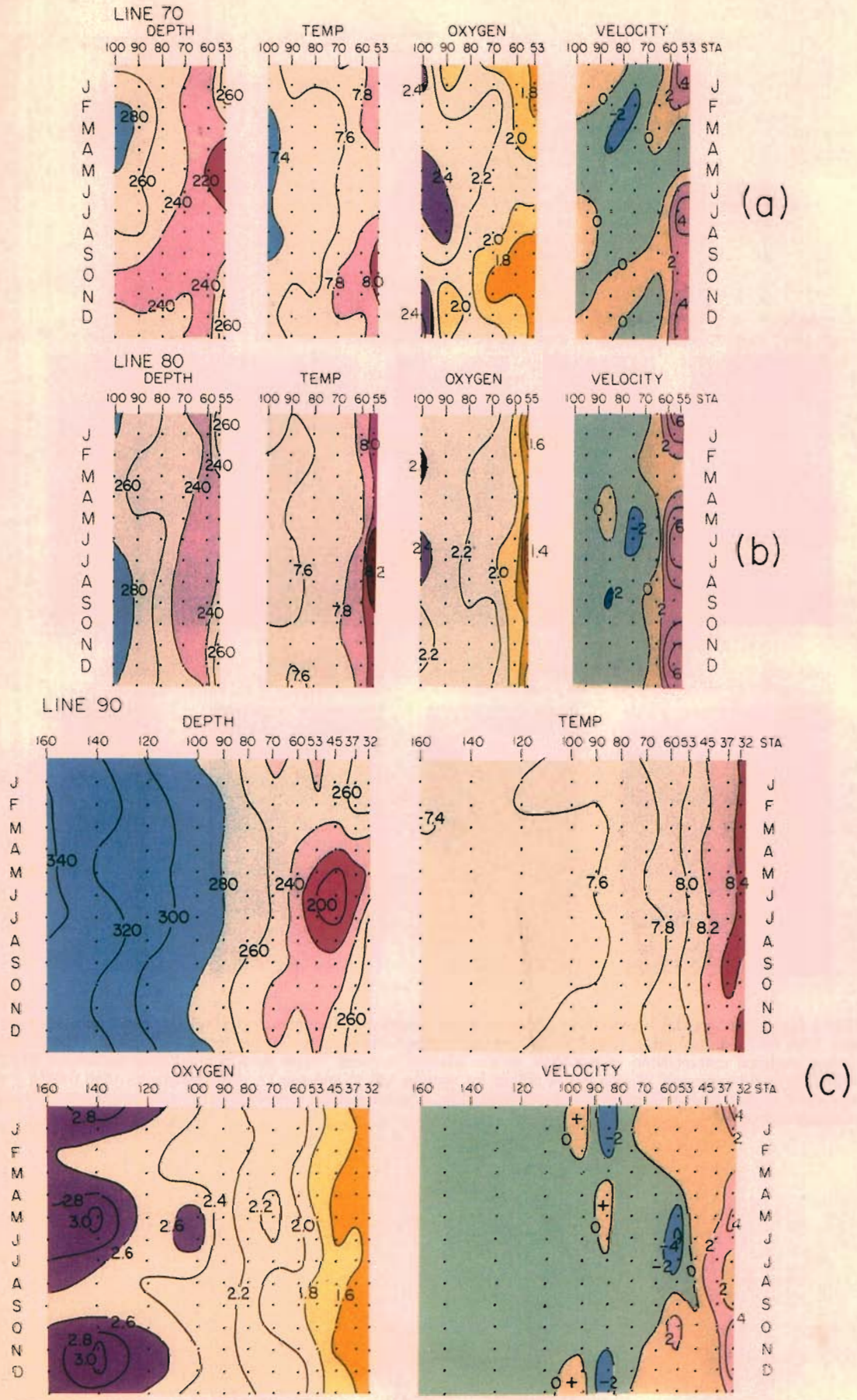

Plate 2 [*Lynn and Simpson*]. Space-time distributions of seasonal mean characteristics for the density surface of σ_t = 26.6 plotted on maps of station position along cardinal lines versus time of year. Extreme values are colored at various intervals.

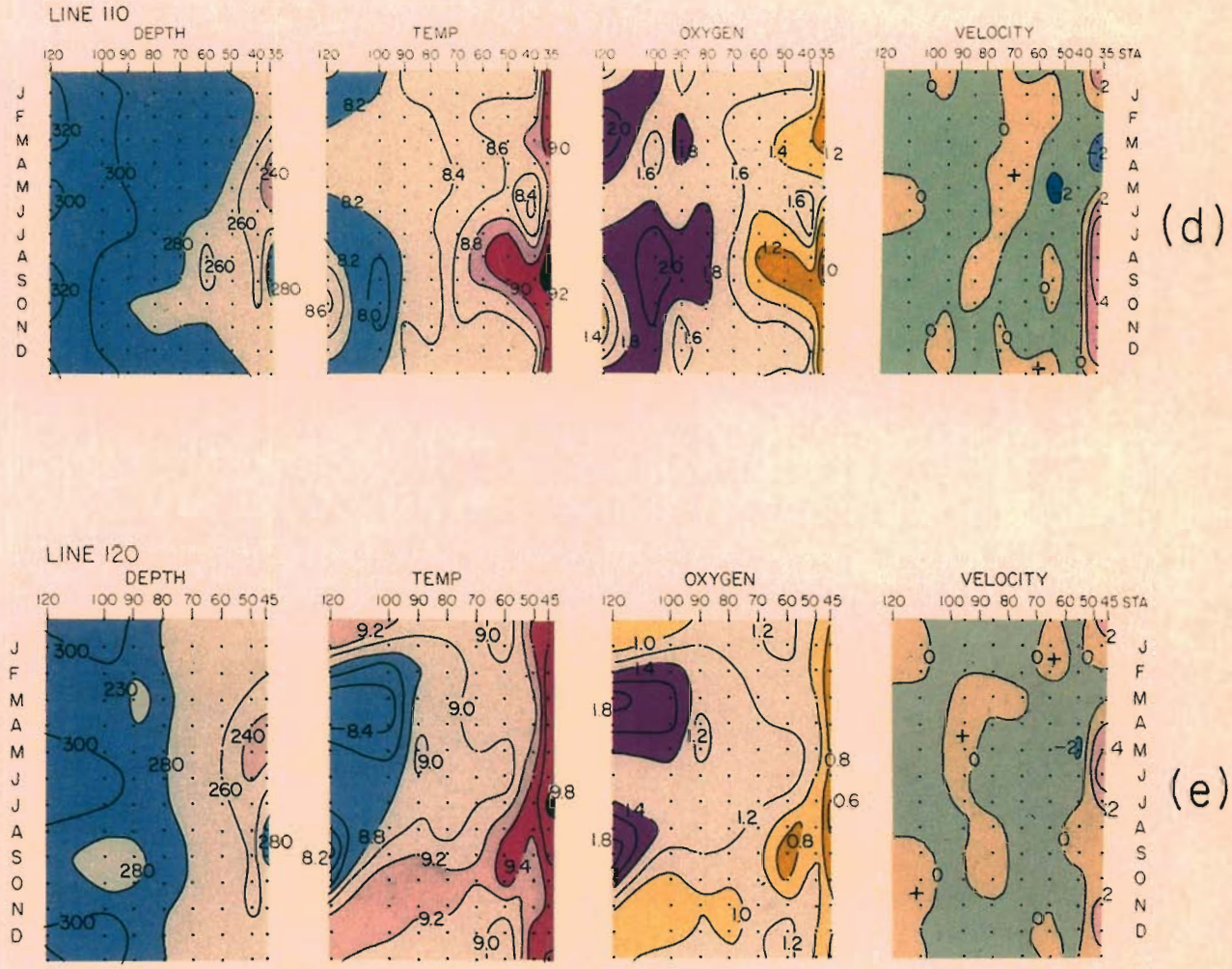

Plate 2 [*Lynn and Simpson*]. (continued)